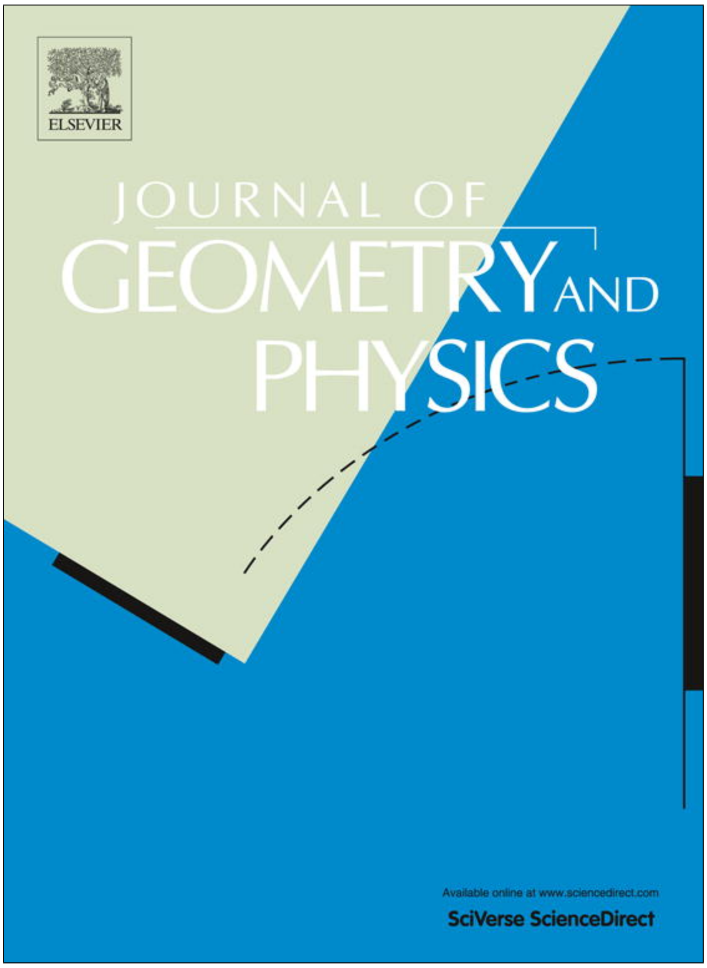
ELSEVIER
JOURNAL OF
GEOMETRY AND
PHYSICS
Available online at www.sciencedirect.com
SciVerse ScienceDirect

Journal of Geometry and Physics 67 (2013) 16–36

Contents lists available at SciVerse ScienceDirect

Journal of Geometry and Physics

journal homepage: www.elsevier.com/locate/jgp

Lie groups, cluster variables and integrable systems

A. Marshakov *

Theory Department, Lebedev Physics Institute, Moscow, Russia
Institute for Theoretical and Experimental Physics, Moscow, Russia
Department of Mathematics, National Research University Higher School of Economics, Moscow, Russia

ARTICLE INFO

Article history:
Received 16 July 2012
Accepted 16 December 2012
Available online 27 December 2012

Keywords:
Integrable systems
Cluster varieties
Poisson–Lie groups

ABSTRACT

We discuss Poisson structures on Lie groups and propose an explicit construction of integrable models on their appropriate Poisson submanifolds. The integrals of motion for the $SL(N)$-series are computed in cluster variables via the Lax map. This construction, when generalised to co-extended loop groups, not only gives rise to several alternative descriptions of relativistic Toda systems but also allows to formulate in general terms some new class of integrable models. We discuss the subtleties of this Lax map in relation to the ambiguity in projection to the trivial co-extension and propose a way to write the spectral curve equation, which fixes this ambiguity, for the periodic Toda chain and its generalisations.

1. Introduction

The relation between integrable systems and Lie groups [1] has many different faces. According to [2], an integrable model can be *directly* constructed on a Poisson submanifold in a Lie group. Integrability in this case follows from the existence of the Ad-invariant functions on a group manifold. Furthermore, this construction can be extended to affine Lie groups [3] and gives rise to a nontrivial wide class of integrable models [4]. It was alternatively discovered that the same class of integrable systems arises from the dimer models on bipartite graphs on a torus [5]. These results partly overlap with and are complementary to the results of [6–9] and closely related studies have also been published [10–12].

For the canonical Poisson structure on a simple Lie group G, we immediately obtain rank$G$ mutually Poisson-commuting functions. Restricting these to a symplectic leaf of dimension $2 \cdot \text{rank}\, G$, we obtain a completely integrable system that is in fact equivalent [2] to a relativistic non-periodic Toda chain [13]. An effective way of constructing the corresponding Poisson submanifold is based on using the cluster coordinates on Lie groups [14–17]. In particular, this allows to compute explicitly the integrals of motion for the $SL(N)$-series. The cluster language also suggests a way to generalise a previous proposal [2] to the case of loop groups and periodic Toda systems, which requires co-extension of the corresponding loop group [3]. This also provides an opportunity to go far beyond this simple relation between Lie groups and the integrable system we start with and to develop a new class of integrable models on the cluster varieties [4], which is important from the point of view of relations with geometry and physics.

In the affine case a nontrivial co-extension is essential, since only the co-extended version of the loop group admits cluster description. However, for construction of an integrable system the total co-extension must be trivial [3,4]. The spectral curve equation in this case is defined ambiguously, so we propose a way to overcome this ambiguity in which the projection on the trivial co-extension is localised to each edge of the exchange graph describing the Poisson submanifold in the loop group. This localisation can only be performed using special coordinates and we discuss their choice for several examples.

* Correspondence to: Theory Department, Lebedev Physics Institute, Moscow, Russia.
E-mail addresses: mars@itep.ru, mars@lpi.ru.

0393-0440/$ – see front matter © 2012 Elsevier B.V. All rights reserved.
doi:10.1016/j.geomphys.2012.12.003

In Section 2 we describe the Poisson submanifolds in Lie groups in terms of the cluster variables. In Section 3 we construct explicitly the integrable system – a relativistic Toda chain – for both simple and co-extended loop groups. The least trivial part of the construction is formulated in Section 3.3 using a localisation procedure for the co-extended loop group. In Section 4 the construction of a relativistic Toda chain is generalised to a wider class of integrable models.

2. Poisson brackets and r-matrices

Let $\mathfrak{g}$ be the Lie algebra of a simple group G, $r \in \mathfrak{g} \otimes \mathfrak{g}$, the standard solution to the (modified) Yang–Baxter equation, that defines a Poisson bracket on the group G according to

$$\{g \underset{,}{\otimes} g\} = -\frac{1}{2}[r, g \otimes g], \tag{2.1}$$

which is compatible with the group structure (see Appendices A and B for notation and some extra formulas concerning r-matrices for the $SL(N)$-series).

The Poisson bracket (2.1) is degenerate on the whole group, but can be restricted on any symplectic leaf of G. A Lie group G can be decomposed into the set of Poisson submanifolds $G^u \subset G$ [17–19] labeled by $u \in W \times W$, where W is the Weyl group of G. The dimension of submanifold G^u is $l(u) + \mathrm{rank}\, G$, where $l(u)$ is the length of the word u, which consists of the generators of the Weyl group W (identified by the set Π of the positive simple roots of G) and the generators of the second copy of W (identified by the set of negative simple roots $\bar{\Pi}$). For our purposes it is more convenient to consider a similar decomposition of the factor $G/\mathrm{Ad}H$ over the Cartan subgroup $H \subset G$; the dimensions of the corresponding symplectic leaves in the factor are just the lengths $l(u)$ themselves.

We can construct a parameterisation of $G^u/\mathrm{Ad}H$ such that the Poisson bracket (2.1) becomes logarithmically constant [17]: for any reduced decomposition $u = \alpha_{i_1} \dots \alpha_{i_l}$ consider the Lax map

$$z_1, \dots, z_l \mapsto E_{i_1} H_{i_1}(z_1) \dots E_{i_l} H_{i_l}(z_l). \tag{2.2}$$

For the group $SL(N)$ on the right-hand side, we can substitute the matrices ($i \in \Pi = \{1, \dots, N-1\}$)

$$H_i(z) = \begin{pmatrix} z & 0 & & \cdots & & 0 \\ 0 & \ddots & & & & 0 \\ & & z & & & \\ \vdots & & & 1 & & \\ & & & & \ddots & 0 \\ 0 & & \cdots & & 0 & 1 \end{pmatrix}, \qquad E_i = \begin{pmatrix} 1 & 0 & & \cdots & & 0 \\ 0 & \ddots & & & & 0 \\ & & 1 & 1 & & \\ \vdots & & & 1 & & \\ & & & & \ddots & 0 \\ 0 & & \cdots & & 0 & 1 \end{pmatrix}, \tag{2.3}$$

where the last line in diagonal $H_i(z)$ with $z \neq 1$ and the only line in E_i containing an off-diagonal value of unity have number i. For negative i the corresponding matrix is transposed to the matrix of the positive root, that is, $E_{\bar{i}} = E_{-i} = E_i^{\mathrm{tr}}$. More precisely, each matrix $H_i(z) \in PGL(N)$ should be normalised for the $SL(N)$ group $H_i(z) \to Z_i = H_i(z)/(\det H_i(z))^{1/N}$ and therefore will always depend on the fractional powers $z^{k/N}$ of the variable z.

The Poisson bracket (2.1) on the parameter z_I is logarithmically constant, that is,

$$\{z_I, z_J\} = \varepsilon_{IJ} z_I z_J, \tag{2.4}$$

where ε_{IJ} is a skew-symmetric matrix that takes integral or half-integral values and acts as the exchange matrix (if group G is simply laced, e.g. $SL(N)$) for the corresponding cluster variety [14–16]. All formulas for symplectic leaves in $G/\mathrm{Ad}H$ can be read from a graph with oriented edges (Appendix C). For the Poisson submanifolds in $G/\mathrm{Ad}H$ we just need consider the graphs on a cylinder instead of a plane. As already pointed out, of particular interest among all G^u are cells corresponding to the Coxeter elements of $W \times W$ with $l(u) = 2 \cdot \mathrm{rank}\, G$.

For the loop groups $\widehat{G}$ one obtains infinitely many Ad-invariant functions, but they still posses finite-dimensional Poisson submanifolds and thus provide a general method for construction of wider classes of integrable models [3]. However, since the Cartan matrices for affine groups (e.g. (A.10)) are non-invertible, for the cluster construction we have to use the co-extended version of loop group $\widehat{G^\sharp}$ [20] instead.

The co-extended affine $\widehat{SL(N)}^\sharp$ can be identified [3,4] with the group

$$A_1(\lambda) T_{z_1} \cdot A_2(\lambda) T_{z_2} = A_1(\lambda) A_2(z_1\lambda) T_{z_1 z_2} \tag{2.5}$$

of expressions $A(\lambda) T_z$, where

$$T_z = \exp\left(\log z \frac{\partial}{\partial \log \lambda}\right) = z^{\lambda \partial/\partial \lambda} \tag{2.6}$$

and $A(\lambda)$ is a Laurent polynomial with values in $N \times N$ matrices. The generators of the co-extended group (labeled now by $i \in \mathbb{Z}_N$) have the form

$$\mathbf{H}_i(z) = H_i(z)T_z, \qquad \mathbf{E}_i = E_i, \qquad \mathbf{E}_{\bar{i}} = E_i^{\rm tr} \tag{2.7}$$

for $i \neq 0$; that is, each corresponding root generator coincides with (2.3), while each Cartan generator is multiplied by the shift operator. For $i = 0$ we also have

$$\mathbf{H}_0(z) = T_z, \qquad \mathbf{E}_0 = \begin{pmatrix} 1 & \cdots & 0 \\ \vdots & \ddots & \vdots \\ \lambda & \cdots & 1 \end{pmatrix}, \qquad \mathbf{E}_{\bar{0}} = \begin{pmatrix} 1 & \cdots & \lambda^{-1} \\ \vdots & \ddots & \vdots \\ 0 & \cdots & 1 \end{pmatrix}. \tag{2.8}$$

It is also useful to introduce the element $\Lambda \in \widehat{SL(N)}$ (as usual, up to normalisation):

$$\Lambda = \begin{pmatrix} 0 & 1 & \cdots & \lambda^{-1} \\ \vdots & \ddots & \ddots & \vdots \\ 0 & \cdots & 0 & 1 \\ 0 & \cdots & 0 & 0 \end{pmatrix} \tag{2.9}$$

with the property

$$\Lambda \mathbf{E}_i \Lambda^{-1} = \mathbf{E}_{i+1}, \qquad \Lambda \mathbf{H}_i(z) \Lambda^{-1} = \mathbf{H}_{i+1}(z), \quad i \in \mathbb{Z}_N. \tag{2.10}$$

This operator acts as a unit shift along the Dynkin diagram. It can also be interpreted as a coextension of the affine Weyl group $\widehat{W}^\sharp$ [4].

We can now consider arbitrarily long words corresponding to the Poisson submanifolds in $\widehat{SL(N)}^\sharp$ of arbitrary large dimensions. However, the space of Ad-invariant functions is infinite only for $\widehat{SL(N)}$, and not for the co-extended group. Therefore, to obtain sufficiently many independent Ad-invariant functions, we have to consider similarly to (2.2) the Lax maps

$$z_1, \ldots, z_l \mapsto \mathbf{E}_{j_1}\mathbf{H}_{j_1}(z_1) \ldots \mathbf{E}_{j_l}\mathbf{H}_{j_l}(z_l) \tag{2.11}$$

into the co-extended loop group, where the parameter z_l must satisfy

$$\prod_j z_j = 1, \qquad \prod_j T_{z_j} = T_{\prod_j z_j} = \mathrm{Id}, \tag{2.12}$$

that is, the total co-extension is trivial. This means that we finally have to project $\widehat{SL(N)}^\sharp \to \widehat{SL(N)}$. The details of this projection are discussed below.

It is easy to understand that exchange graphs for symplectic leaves in $SL(N)$ and Poisson submanifolds in loop groups $\widehat{SL(N)}$ can be constructed by gluing the rhombi (Fig. 1, Appendix C) on a cylinder for the simple group and on a torus for the loop group case. The graphs for $SL(N)$ have $N - 1$ vertical levels (the corresponding upper and lower rhombi are cut into triangles) and are glued in the horizontal direction, while the graphs for the Poisson submanifolds of the same dimension in $\widehat{SL(N)}$ have one extra level (for the same N) and are periodic in the vertical direction as well. This construction is illustrated by explicit examples in the next section.

3. Integrable system

It is easy to see directly from (2.1) that any two Ad-invariant functions on G Poisson-commute with each other. For example, in the simply laced case, when the r-matrix is

$$r = \sum_{\alpha \in \Delta_+} e_\alpha \wedge e_{\bar{\alpha}} = \sum_{\alpha \in \Delta_+} (e_\alpha \otimes e_{\bar{\alpha}} - e_{\bar{\alpha}} \otimes e_\alpha) \tag{3.1}$$

(the sum is taken over the set of all positive roots Δ_+ of Lie group G), the Poisson bracket is given by

$$\{\mathcal{H}_1, \mathcal{H}_2\} = -\frac{1}{2} \sum_{\alpha \in \Delta_+} \left(L_{e_\alpha}\mathcal{H}_1 L_{e_{\bar{\alpha}}}\mathcal{H}_2 - R_{e_\alpha}\mathcal{H}_1 R_{e_{\bar{\alpha}}}\mathcal{H}_2 \right), \tag{3.2}$$

where L_v (R_v) denotes the corresponding left (right) vector field for any $v \in \mathfrak{g}$. Any Ad-invariant function $\mathcal{H}$ satisfies $L_v\mathcal{H} = -R_v\mathcal{H}$ and thus the bracket (3.2) of two such functions vanishes. The bracket (3.2) obviously vanishes even if the functions are defined not on the whole G, but on any Poisson Ad-invariant subvariety of G.

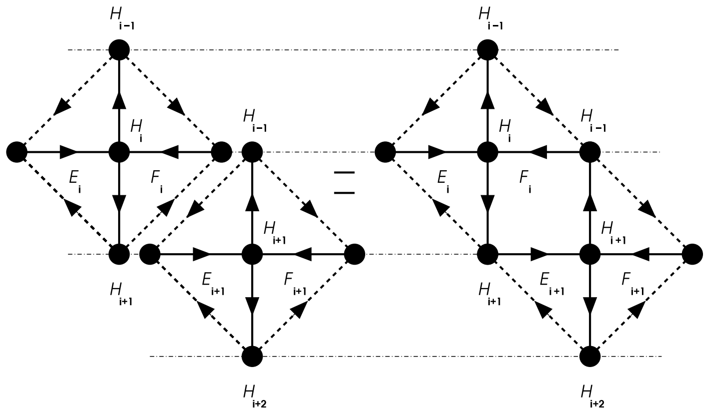

Fig. 1. Graphs depicting the Poisson submanifolds in $SL(N)$ generated by the positive simple roots E_i and negative roots $E_{\bar{i}}$, $1 < i < N-1$, or the submanifolds in $\widehat{SL(N)}$ for $i \in \mathbb{Z}_N$. Gluing of two such graphs yields an element of the two-dimensional square lattice.

On a simple group there exists rank G independent Ad-invariant functions. A possible basis of these functions is the set $\{\mathcal{H}_i\}$ for $i \in \Pi$ (the set of positive simple roots $\Pi \subset \Delta_+$):

$$\mathcal{H}_i = \mathrm{Tr}\, \pi_{\mu_i}(g), \tag{3.3}$$

where π_{μ_i} is the ith fundamental representation of G with the highest weight $(\mu_i, \alpha_j) = \delta_{ij}$ dual to α_i, $i \in \Pi$. These functions then define an integrable system on a symplectic leaf of dimension $2 \cdot \mathrm{rank}\, G$. It has been shown [2] that they form the set of integrals of motion for the open relativistic Toda chain [13], with the canonical Hamiltonian for the $SL(N)$-series

$$\mathcal{H} = \mathcal{H}_1 + \mathcal{H}_{N-1} = \mathrm{Tr}\left(g + g^{-1}\right) = \sum_{i=1}^{N} (\exp(p_i) + \exp(-p_i)) \sqrt{1 + \exp(q_i - q_{i+1})}\sqrt{1 + \exp(q_{i-1} - q_i)}. \tag{3.4}$$

The more well-known canonical (non-relativistic) Toda system is recovered in the limit from the Lie group to Lie algebra (Appendix D).

3.1. Simple group: examples

$SL(2)$. On a symplectic leaf of a two-particle relativistic Toda, corresponding to the word $u = \alpha_1 \alpha_{\bar{1}}$, we can choose the following parameterisation:

$$g(x, y) \simeq Y^{1/2} E X \bar{E} Y^{1/2} \simeq Y E X \bar{E} \simeq E X \bar{E} Y = \frac{1}{\sqrt{xy}} \begin{pmatrix} xy + y & 1 \\ y & 1 \end{pmatrix}, \tag{3.5}$$

where

$$\begin{aligned}
&Y = H(y)/\det H(y)^{1/2} = \begin{pmatrix} y^{1/2} & 0 \\ 0 & y^{-1/2} \end{pmatrix}, \\
&X = H(x)/\det H(x)^{1/2} = \begin{pmatrix} x^{1/2} & 0 \\ 0 & x^{-1/2} \end{pmatrix} \\
&E = \begin{pmatrix} 1 & 1 \\ 0 & 1 \end{pmatrix}, \qquad \bar{E} = \begin{pmatrix} 1 & 0 \\ 1 & 1 \end{pmatrix}.
\end{aligned} \tag{3.6}$$

Expansion (3.5) (refinement of the Gauss decomposition) corresponds to the graph $y \to x \leftarrow y$ with three vertices and two edges. Identification of the ends leads to $y \Rightarrow x$, inducing the Poisson structure

$$\{y, x\} = 2yx. \tag{3.7}$$

The cluster variables are related to the Darboux coordinates by

$$x = e^{-q}, \qquad y = \frac{e^{2p}}{1 + x} \tag{3.8}$$

while the Hamiltonian (only in this example) is

$$\mathcal{H} = \mathrm{Tr}\, g(x, y) = \sqrt{xy} + \sqrt{\frac{y}{x}} + \frac{1}{\sqrt{xy}} = \left(e^p + e^{-p}\right)\sqrt{1 + e^q}, \tag{3.9}$$

the canonical Hamiltonian (3.4) for the two-particle open system.

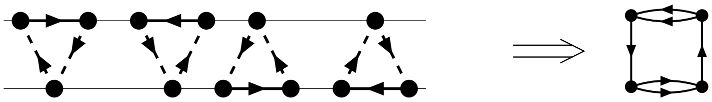

Fig. 2. Construction of a graph for the word $1\bar{1}2\bar{2}$ in $SL(3)$. The triangles are just cut rhombi from Fig. 1 (see also Fig. 11). Gluing of these triangles and the left and right ends for $SL(3)/\mathrm{Ad}H$ yields the plot on the right with the exchange matrix constructed from the Cartan matrix (3.14).

$SL(3)$. For the group $SL(3)$, formula (2.2) gives

$$g(\mathbf{x},\mathbf{y}) = \underbrace{E_1 X_1 E_{\bar{1}} Y_1}_{g_1} \cdot \underbrace{E_2 X_2 E_{\bar{2}} Y_2}_{g_2}, \tag{3.10}$$

where

$$E_1 = E_{\bar{1}}^{\mathrm{tr}} = \begin{pmatrix} 1 & 1 & 0 \\ 0 & 1 & 0 \\ 0 & 0 & 1 \end{pmatrix}, \qquad E_2 = E_{\bar{1}}^{\mathrm{tr}} = \begin{pmatrix} 1 & 1 & 0 \\ 0 & 1 & 0 \\ 0 & 0 & 1 \end{pmatrix} \tag{3.11}$$

and the normalised Cartan elements are

$$\begin{aligned} &Y_i = H_i(y_i) / \det H_i(y_i)^{1/3}, \qquad X_i = H_i(x_i) / \det H_i(x_i)^{1/3}, \qquad i = 1, 2 \\ &H_1(z) = \begin{pmatrix} z & 0 & 0 \\ 0 & 1 & 0 \\ 0 & 0 & 1 \end{pmatrix}, \qquad H_2(z) = \begin{pmatrix} z & 0 & 0 \\ 0 & z & 0 \\ 0 & 0 & 1 \end{pmatrix}. \end{aligned} \tag{3.12}$$

The variables $\mathbf{x}$ and $\mathbf{y}$ correspond to the vertices of the graph $\begin{smallmatrix} x_1 \\ y_2 \end{smallmatrix} \downarrow \begin{smallmatrix} \Leftarrow \\ \Rightarrow \end{smallmatrix} \uparrow \begin{smallmatrix} y_1 \\ x_2 \end{smallmatrix}$, constructed from glued cut-rhombus triangles (Fig. 2) and satisfy the following Poisson bracket relations:

$$\{y_i, x_j\} = C_{ij} y_i x_j, \quad i, j = 1, 2 \tag{3.13}$$

with the Cartan matrix of $\mathfrak{g} = sl_3$

$$\|C_{ij}\| = \begin{pmatrix} 2 & -1 \\ -1 & 2 \end{pmatrix}, \qquad \|C_{ij}^{-1}\| = \begin{pmatrix} 2/3 & 1/3 \\ 1/3 & 2/3 \end{pmatrix}. \tag{3.14}$$

To obtain the integrals of motion, consider the characteristic polynomial for (3.10):

$$\det\left(\mu + g(\mathbf{x},\mathbf{y})\right) = \mu^3 + \mathcal{H}_2(\mathbf{x},\mathbf{y})\mu^2 + \mathcal{H}_1(\mathbf{x},\mathbf{y})\mu + 1, \tag{3.15}$$

where (with C_{jk}^{-1} the inverse Cartan matrix from (3.14))

$$\begin{aligned} \mathcal{H}_1(\mathbf{x},\mathbf{y}) &= \mathrm{Tr}\, g^{-1} = \prod_k (x_k y_k)^{-C_{1k}^{-1}} \cdot (1 + y_1 + y_1 x_1 + y_1 x_1 y_2 + y_1 x_1 y_2 x_2) \\ \mathcal{H}_2(\mathbf{x},\mathbf{y}) &= \mathrm{Tr}\, g = \prod_k (x_k y_k)^{-C_{2k}^{-1}} \cdot (1 + y_2 + y_2 x_2 + y_2 x_2 y_1 + y_2 x_2 y_1 x_1) \end{aligned} \tag{3.16}$$

become two integrals of motion $\{\mathcal{H}_1, \mathcal{H}_2\} = 0$ for the Poisson bracket (3.13).

3.2. Cluster variables and the $SL(N)$ chain

Explicit formulas can easily be written for generic $G = SL(N)$. The product (2.2) becomes

$$\begin{aligned} &g(\mathbf{x},\mathbf{y}) = \underbrace{E_1 X_1 E_{\bar{1}} Y_1}_{g_1} \cdot \underbrace{E_2 X_2 E_{\bar{2}} Y_2}_{g_2} \cdot \ldots \cdot \underbrace{E_{N-1} X_{N-1} E_{\overline{N-1}} Y_{N-1}}_{g_{N-1}} \\ &Y_i = H_i(y_i) / \det H_i(y_i)^{1/N}, \qquad X_i = H_i(x_i) / \det H_i(x_i)^{1/N}, \qquad i = 1, \ldots, N-1 \end{aligned} \tag{3.17}$$

with notation according to (2.3). The corresponding graph $\begin{smallmatrix} y_1 \\ x_1 \end{smallmatrix} \Downarrow \begin{smallmatrix} \leftarrow \\ \rightarrow \end{smallmatrix} \Uparrow \begin{smallmatrix} x_2 \rightarrow \\ y_2 \leftarrow \end{smallmatrix} \Downarrow \begin{smallmatrix} y_3 \leftarrow \\ x_3 \rightarrow \end{smallmatrix} \ldots \begin{smallmatrix} \rightarrow \\ \leftarrow \end{smallmatrix} \Downarrow \begin{smallmatrix} y_{N-1} \\ x_{N-1} \end{smallmatrix}$ induces the Poisson bracket

$$\{y_i, x_j\} = C_{ij} y_i x_j, \quad i, j = 1, \ldots, N-1 \tag{3.18}$$

with the $\mathfrak{g} = sl_N$ Cartan matrix (A.1). Computing the product in (3.17) yields the Lax operator, and its characteristic polynomial

$$\det\left(\mu + g(\mathbf{x},\mathbf{y})\right) = \sum_{j=0}^{N} \mu^j \mathcal{H}_j(\mathbf{x},\mathbf{y}) \tag{3.19}$$

generates rank $SL(N) = N-1$ nontrivial ($\mathcal{H}_0 = \mathcal{H}_N = 1$ in the accepted normalisation, and $\mathcal{H}_1 = \mathrm{Tr}\, g^{-1}$, $\mathcal{H}_{N-1} = \mathrm{Tr}\, g$) Poisson-commuting (w.r.t. the bracket (3.18)) integrals of motion $\{\mathcal{H}_i, \mathcal{H}_j\} = 0,\ i,j = 1,\ldots,N-1$, which are

$$\mathcal{H}_j(\mathbf{x},\mathbf{y}) = \prod_k (x_k y_k)^{-C^{-1}_{jk}} \cdot Z_j(\mathbf{x},\mathbf{y}). \tag{3.20}$$

The Lax map (2.2) allows us to compute explicitly the polynomials

$$Z_j(\mathbf{x},\mathbf{y}) = \sum_{0\le m_i\le \max(i,N-1-i)}^{m_j\ge m_{j\pm1}\ge m_{j\pm2}\ge\ldots} \sum_{m_i-1\le n_i\le m_i} \prod_i y_i^{m_i} x_i^{n_i}, \tag{3.21}$$

which all have unit coefficients.

The Darboux coordinates are related to the cluster variables by

$$x_i = \exp(-(\alpha_i\cdot q)), \qquad y_i = \exp((\alpha_i\cdot P) + (\alpha_i\cdot q)), \quad i = 1,\ldots,N-1 \tag{3.22}$$

with the "long momentum" (cf. the canonical transformation used in [21])

$$P = p - \frac{1}{2}\sum_{k=1}^{N-1}\alpha_k \log\left(1+\exp(\alpha_k\cdot q)\right) = p + \frac{\partial}{\partial q}\left(\frac{1}{2}\sum_{k=1}^{N-1}\mathrm{Li}_2\left(-\exp(\alpha_k\cdot q)\right)\right), \tag{3.23}$$

where the $(N-1)$-vectors q and p denote the canonical coordinate and momentum in the center-of-mass frame. Substituting (3.22) into the expression $\mathcal{H} = \mathcal{H}_1 + \mathcal{H}_{N-1}$ yields the canonical Toda Hamiltonian (3.4), where (in the open case, in contrast to the periodic chain considered below) we have to drop off the square roots with α_0 and α_N, that is, replace $\sqrt{1+\exp(q_0-q_1)}$ and $\sqrt{1+\exp(q_N-q_{N+1})}$ by unities.

3.3. Loop group $\widehat{SL(N)}$ and the N-periodic chain

The proposed approach does not only work for finite-dimensional Lie groups [3]. It is almost obvious that to obtain the periodic Toda chain we should consider decomposition (2.11) for loop groups containing an extra affine simple root, that is, $u = \alpha_0\bar\alpha_0\alpha_1\bar\alpha_1\ldots\alpha_{N-1}\bar\alpha_{N-1} \in \hat W \times \hat W$. At the level of Lie algebras (Appendix D) this obviously gives rise to the well-known spectral-parameter-dependent Lax matrix (D.4) in the evaluation representation of the corresponding affine algebra. For relativistic Toda, instead of using the cluster formulation of the co-extended loop group $\widehat{SL(N)}^\sharp$, we construct a Poisson submanifold in $\widehat{SL(N)}/\mathrm{Ad}H$, but fixing the spectral parameter now becomes a nontrivial issue. It depends on a particular way of locating the shift operators in (2.11): the total co-extension must be trivial because of (2.12), and all shift operators can be "annihilated", say, by moving them all to the right.

Note that when moving the shift operator (2.6) through a spectral-parameter-dependent matrix corresponding to the affine root, we multiply the spectral parameter by the dynamical variable. This results in nontrivial multiplicative renormalisation of the coefficients of the spectral curve equation. In particular, it means that the coefficients themselves are defined ambiguously and only their invariant combinations can be the Poisson-commuting quantities [3,4]. However, we propose here a localising prescription that completely overcomes this ambiguity (Section 4.1).

For the group $\widehat{SL(N)}^\sharp$ the (normalised to unit determinant) product (2.2) for the word $u = \prod_{j\in\mathbb{Z}_N}\alpha_j\bar\alpha_j$ can be written as

$$\begin{aligned} g(\lambda|\mathbf{x},\mathbf{y}) &= \prod_{j\in\mathbb{Z}_N}\mathbf{E}_j\mathbf{H}_j(x_j)\mathbf{E}_{\bar j}\mathbf{H}_j(y_j) = \prod_{j\in\mathbb{Z}_N}\mathbf{E}_jX_jT_{x_j}\mathbf{E}_{\bar j}Y_jT_{y_j} \\ &= \prod_{j\in\mathbb{Z}_N}\mathbf{E}_jX_jT_{x_{\nu_j}}T^{-1}_{x_{\nu_{j+1}}}\mathbf{E}_{\bar j}Y_jT_{y_{\nu_j}}T^{-1}_{y_{\nu_{j+1}}}. \end{aligned} \tag{3.24}$$

The new variables z_{ν_j}, $j\in\mathbb{Z}_N$, are introduced by $z_j = z_{\nu_j}/z_{\nu_{j+1}}$ (see definition (A.4)). Instead of moving all the shift operators to the right, we choose the following prescription:

$$g(\lambda|\mathbf{x},\mathbf{y}) \simeq \prod_{j\in\mathbb{Z}_N} T^{-1}_{y_{\nu_j}}\mathbf{E}_jX_jT_{x_{\nu_j}}T^{-1}_{x_{\nu_{j+1}}}\mathbf{E}_{\bar j}Y_jT_{y_{\nu_j}} \simeq \prod_{j\in\mathbb{Z}_N} T^{-1}_{x_{\nu_j}}T^{-1}_{y_{\nu_j}}\mathbf{E}_jX_jT_{x_{\nu_j}}\mathbf{E}'_{\bar j}Y_jT_{y_{\nu_j}}, \tag{3.25}$$

where $\simeq$ denotes an equality modulo cyclic permutation, and clearly

$$\begin{aligned} &\mathbf{E}'_{\bar j} = \mathbf{E}_{\bar j} = E_{\bar j}, \qquad \mathbf{E}'_{\bar 0} = \mathbf{E}_{\bar 0}(\lambda/x_{\nu_{j+1}}) \\ &Y_j = H_j(y_j)/\det H_j(y_j)^{1/N}, \qquad X_j = H_j(x_j)/\det H_j(x_j)^{1/N}, \quad j = 1,\ldots,N-1. \end{aligned} \tag{3.26}$$

All factors under the product on the right-hand side of (3.25) do not in fact contain shift operators, since

$$T^{-1}_{x_{\nu_j}}T^{-1}_{y_{\nu_j}}E_jX_jT_{x_{\nu_j}}E_{\bar j}Y_jT_{y_{\nu_j}} = E_jX_jE_{\bar j}Y_j, \quad j = 1,\ldots,N-1 \tag{3.27}$$

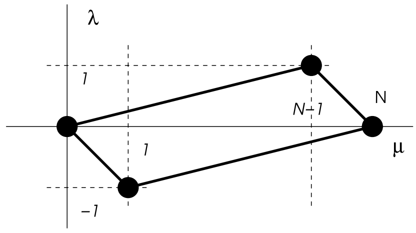

Fig. 3. Newton polygon for the N-periodic Toda equation (3.33). The marked boundary points correspond to the Casimir functions, which are unity in the normalised Eq. (3.33), while the internal points on the horizontal axis correspond to the integrals of motion.

and

$$\begin{aligned} T_{x_{\nu_0}}^{-1} T_{y_{\nu_0}}^{-1} \mathbf{E}_0 T_{x_{\nu_0}} \mathbf{E}'_{\bar{0}} T_{y_{\nu_0}} &= \mathbf{E}_0 \left(\frac{\lambda}{x_{\nu_0} y_{\nu_0}} \right) \mathbf{E}_{\bar{0}} \left(\frac{\lambda}{y_{\nu_0} x_{\nu_1}} \right) \\ &= \mathbf{E}_0 \left(\lambda x_{\mu_{N-1}} y_{\mu_{N-1}} \right) \mathbf{E}_{\bar{0}} \left(\frac{\lambda y_{\mu_{N-1}}}{x_{\mu_1}} \right) \equiv \mathfrak{g}_0(\lambda). \end{aligned} \tag{3.28}$$

That is, on the right-hand side of (3.25) we obtain a product of matrices in the evaluation representation of $\widehat{SL(N)}$. Hence, starting initially with the co-extended loop group $\widehat{SL(N)}^\sharp$, which has a cluster description, we have found a way to construct explicitly the Poisson submanifold in $\widehat{SL(N)}/\mathrm{Ad}H$ in terms of the product of $\widehat{SL(N)}$-valued factors only. To do this we actually have to change the coordinates. The weight variables in (3.28) can be explicitly defined as

$$x_{\mu_j} = \prod_k x_k^{C_{jk}^{-1}}, \qquad y_{\mu_j} = \prod_k y_k^{C_{jk}^{-1}}, \quad j = 1, \dots, N-1, \tag{3.29}$$

where C_{jk}^{-1} is the inverse Cartan matrix for $\mathfrak{g} = sl_N$ (Appendix A). Finally, we obtain the Lax map

$$g(\lambda|\mathbf{x}, \mathbf{y}) \simeq \mathfrak{g}_0(\lambda) \cdot g_N(\mathbf{x}, \mathbf{y}), \tag{3.30}$$

where the matrix $g_N(\mathbf{x}, \mathbf{y})$ is constructed in (3.17) for the open chain.

By the standard rules, the Poisson brackets coming from the graph on the torus

$$\{y_i, x_j\} = \hat{C}_{ij} y_i x_j, \quad i, j \in \mathbb{Z}_N \tag{3.31}$$

are defined by (degenerate) Cartan matrix (A.10) of the affine $\mathfrak{g} = \widehat{sl}_N$, with the Casimir function

$$\mathcal{C} = \prod_{j \in \mathbb{Z}_N} x_j = \prod_{j \in \mathbb{Z}_N} y_j^{-1}. \tag{3.32}$$

Fixing the value of the Casimir (3.32), one gets a description of the corresponding Poisson submanifold (of dimension $2(N-1)$) in terms of the non-degenerate Poisson structure (3.18) of the open chain.

Vanishing of the characteristic polynomial for (3.24) (Fig. 3),

$$\det(\mu + g(\lambda|\mathbf{x}, \mathbf{y})) = \sum_{j=0}^{N} \mu^j \mathcal{H}_j(\mathbf{x}, \mathbf{y}) + \mu^{N-1}\lambda + \frac{\mu}{\lambda}, \tag{3.33}$$

can be rewritten in the standard form of the relativistic Toda spectral curve equation [22–24]:

$$\begin{aligned} &w + \frac{1}{w} = P_N(z) = z^{-N/2} \sum_{j=0}^{N} z^j (-)^{N-j} \mathcal{H}_j(\mathbf{x}, \mathbf{y}) \\ &z = -\mu, \qquad w = \lambda z^{N/2-1} \end{aligned} \tag{3.34}$$

with the two meromorphic differentials $\frac{dz}{z}$ and $\frac{dw}{w}$ having all fixed periods on the curve (3.34). Formulas (3.33) and (3.34) define (in addition to the constant Casimirs $\mathcal{H}_0 = \mathcal{H}_{N-1} = 1$) the set of independent Poisson-commuting integrals of motion

$$\{\mathcal{H}_j, \mathcal{H}_k\} = 0, \quad j, k = 1, \dots, N-1 \tag{3.35}$$

with respect to the bracket (3.18). The canonical Hamiltonian of the integrable system is still given by (3.4), where the terms with $\alpha_0 = \alpha_N$ are no longer dropped.

The Darboux coordinates are introduced again by the transformation

$$x_i = \exp(-(\alpha_i \cdot q)), \qquad y_i = \exp(\alpha_i \cdot (P + q)), \quad i \in \mathbb{Z}_N, \tag{3.36}$$

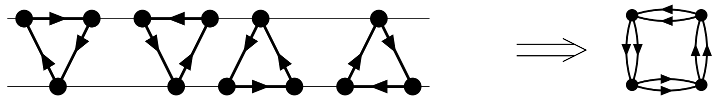

Fig. 4. Example of a graph for the word $0\bar{0}1\bar{1}$ for $\widehat{SL(2)}/\mathrm{Ad}H$. In contrast to Fig. 2, the arrows connecting two levels, two simple roots of $\widehat{SL(2)}$, are solid lines. After gluing, the image on the right shows the structure of the degenerate Cartan matrix of $\mathfrak{g} = \widehat{sl}_2$.

which is valid for the extended set of roots. Now, instead of (3.23) we obtain

$$P = p + \frac{1}{2}\sum_{k=1}^{N-1}\alpha_k \log\frac{1+\exp(\alpha_N\cdot q)}{1+\exp(\alpha_k\cdot q)} = p + \frac{\partial}{\partial q}\left(\frac{1}{2}\sum_{k=1}^{N}\mathrm{Li}_2\left(-\exp(\alpha_k\cdot q)\right)\right), \tag{3.37}$$

where the canonical transformation is again generated by di-logarithm functions.

Example of $\widehat{SL(2)}$. We simply take the map (2.11) of the word $0\bar{0}1\bar{1}$ into $\widehat{SL(2)}/\mathrm{Ad}H$. According to Fig. 4, the parameterisation can be read from the graph $\Downarrow_{y_0 \Rightarrow x_0}^{x \Leftarrow y} \Uparrow$ with four variables in the vertices satisfying

$$\{y, x\} = 2yx \tag{3.38}$$

as in the "open" $SL(2)$ case, completed now by

$$\{y_0, x\} = -2y_0 x, \qquad \{y, x_0\} = -2yx_0, \qquad \{y, y_0\} = \{x, x_0\} = 0. \tag{3.39}$$

The structure of the Poisson brackets (3.38) and (3.39) is encoded in the degenerate Cartan matrix (A.10) of $\mathfrak{g} = \widehat{sl}_2$ and the product $\mathcal{C} = xx_0 = \frac{1}{yy_0}$ is the Casimir function. The only nontrivial integral of motion in this example,

$$\mathcal{H} = \frac{1 + y + xy + \mathcal{C}^{-1}x}{\sqrt{xy}} = \left(e^p + e^{-p}\right)\sqrt{1+\exp(q)}\sqrt{1+\mathcal{C}^{-1}\exp(-q)}, \tag{3.40}$$

is the Hamiltonian of the periodic two-particle chain (3.4) on

$$x = \exp(-q), \qquad y = \exp(2p+q)\frac{1+\mathcal{C}^{-1}e^{-q}}{1+e^q}. \tag{3.41}$$

Example of $\widehat{SL(3)}$. In this case the characteristic polynomial (3.33) or the spectral curve equation (3.34) gives two nontrivial integrals of motion,

$$\begin{aligned}
\mathcal{H}_1 &= \prod_k (x_k y_k)^{-C^{-1}_{1k}} \cdot \left(1 + y_1 + y_1x_1 + y_1x_1y_2 + y_1x_1y_2x_2 + \mathcal{C}^{-1}x_1x_2\right) \\
\mathcal{H}_2 &= \prod_k (x_k y_k)^{-C^{-1}_{2k}} \cdot \left(1 + y_2 + y_2x_2 + y_2x_2y_1 + y_2x_2y_1x_1 + \mathcal{C}^{-1}x_1x_2\right),
\end{aligned} \tag{3.42}$$

expressed in terms of the independent variables using the Casimir relation $\mathcal{C} = x_0x_1x_2 = \frac{1}{y_0y_1y_2}$. Only the last terms on the right-hand sides of (3.42) differ from the Hamiltonians of non-periodic chain (3.16).

3.4. Mutations and discrete flows

The *discrete* transformations that leave the Toda integrals of motion invariant are constructed as a sequence of mutations (see (C.6)) of the corresponding graphs. For (3.20) and (3.21) these are

$$\tilde{y}_i^{-1} = y_i \prod_j \left(1 + x_j^{\mathrm{sgn}(C_{ij})}\right)^{-C_{ij}}, \qquad \tilde{x}_i = x_i^{-1}\prod_j\left(1 + \tilde{y}_j^{-\mathrm{sgn}(C_{ij})}\right)^{C_{ij}} \tag{3.43}$$

from mutations of the graph ${}^{y_1}_{x_1}\Downarrow^{\leftarrow}_{\rightarrow} \Uparrow {}^{x_2\rightarrow}_{y_2\leftarrow}\Downarrow^{y_3\leftarrow}_{x_3\rightarrow} \ldots {}^{\rightarrow}_{\leftarrow}\Downarrow^{y_{N-1}}_{x_{N-1}}$. For example, the Hamiltonians (3.16) are invariant under the transformations[1]

$$\begin{aligned}
\tilde{y}_1 &= \frac{1}{y_1}(1+x_1)^{-2}\left(1+\frac{1}{x_2}\right), \qquad \tilde{y}_2 = \frac{1}{y_2}(1+x_2)^{-2}\left(1+\frac{1}{x_1}\right) \\
\tilde{x}_1 &= \frac{1}{x_1}\left(1+\frac{1}{\tilde{y}_1}\right)^2(1+\tilde{y}_2)^{-1}, \qquad \tilde{x}_2 = \frac{1}{x_2}\left(1+\frac{1}{\tilde{y}_2}\right)^2(1+\tilde{y}_1)^{-1},
\end{aligned} \tag{3.45}$$

---

[1] In the dual variables $x_j = \prod_k b_k^{C_{jk}}$ and $y_j = \prod_k a_k^{-C_{jk}}$ they acquire the form of the discrete bilinear Hirota equations

$$\begin{aligned}
a_i\tilde{a}_i &= b_i^2 + b_{i+1}b_{i-1} \\
b_i\tilde{b}_i &= \tilde{a}_i^2 + \tilde{a}_{i+1}\tilde{a}_{i-1}
\end{aligned} \tag{3.44}$$

with $b_0 = b_3 = a_0 = a_3 = 2$ for $SL(3)$, for example.

leaving invariant the graph ${}^{x_1}_{y_2}\downarrow\substack{\Leftarrow\\ \Rightarrow}\uparrow{}^{y_1}_{x_2}$. The affine Toda Hamiltonians (3.33) and (3.34) are correspondingly preserved by

$$\tilde{y}_i^{-1} = y_i \prod_j \left(1 + x_j^{\mathrm{sgn}(\hat{C}_{ij})}\right)^{-\hat{C}_{ij}}, \qquad \tilde{x}_i = x_i^{-1} \prod_j \left(1 + \tilde{y}_j^{-\mathrm{sgn}(\hat{C}_{ij})}\right)^{\hat{C}_{ij}} \tag{3.46}$$

from similar mutations of the graph with the exchange matrix constructed from $\hat{C}_{ij}$ (A.10).

These transformations can be considered as discrete flows in the spirit of Hoffman et al. [19]. For example, in the decomposition (3.5) into the product of upper-triangular and lower-triangular matrices we change the order, that is,

$$\begin{aligned} g(x, y) \simeq g_+(x, y) \cdot g_-(x, y) &\simeq H(y)EH(x)F \\ &= H(y)H(1 + x)FH(x^{-1})EH(1 + x) \simeq H\left(y(1 + x)^2\right) FH\left(x^{-1}\right) E \\ &\simeq \tilde{g}_-\left(\tilde{x}, \tilde{y}\right) \cdot \tilde{g}_+\left(\tilde{x}, \tilde{y}\right) \end{aligned} \tag{3.47}$$

where we use commutation relations previously described [17]. The decomposition on the right-hand side in "reverse order" corresponds to changing coordinates by the sequence of mutations

$$\left(\tilde{y}, \tilde{x}\right) = \mu_{y(1+x)^2}\left(y(1 + x)^2, x^{-1}\right) \circ \mu_x(y, x) = \left(y^{-1}(1 + x)^{-2}, x^{-1}(1 + y(1 + x)^2)^2\right) \tag{3.48}$$

for the graph $x \Leftarrow y$. Note that as usual we consider the product in (3.47) for modulo cyclic permutations and conjugation by a Cartan element, since only the Ad-invariant functions are essential for our purposes. The same is certainly true for the "reflected composition", when we first make mutation in y- and then in x-vertices of the exchange graph.

4. Towards a new class of integrable models

We have already pointed out that loop groups allow us to construct a much wider class of integrable systems [3,4]. We demonstrate this here using just a few examples, starting from the well-known "dual" representation for the Toda chains [25].

4.1. 2×2 formulation for the relativistic N-particle Toda

The same graph $\Downarrow^{x\,\Leftarrow\,y}_{y_0\,\Rightarrow\,x_0}\Uparrow$ for the $\widehat{SL(2)}$ Toda system (when rotated clockwise, i.e. $\Downarrow^{y_0\,\Leftarrow\,x}_{x_0\,\Rightarrow\,y}\Uparrow = {}_{x_0}\downarrow\substack{\leftarrow\\ \rightarrow}\uparrow^{x}_{y}\uparrow\substack{\rightarrow\\ \leftarrow}\downarrow^{y_0}$) can be associated with another decomposition,

$$\begin{aligned} \mathbf{H}_0(x_0)\mathbf{E}_0\mathbf{E}_{\bar{1}}\mathbf{H}_0(y)\mathbf{H}_1(x)\mathbf{E}_{\bar{0}}\mathbf{E}_1\mathbf{H}_1(y_0) &\simeq \mathbf{H}_0(x_0)\mathbf{E}_0\omega\mathbf{E}_{\bar{0}}\mathbf{H}_1(y) \cdot \mathbf{H}_0(x)\mathbf{E}_0\omega\mathbf{E}_{\bar{0}}\mathbf{H}_1(y_0) \equiv \\ &\equiv \Xi(x_0, y) \cdot \Xi(x, y_0), \end{aligned} \tag{4.1}$$

where $\simeq$ denotes equality modulo cyclic permutation. Here

$$\begin{aligned} \Xi(x, y) &= \mathbf{H}_0(x)\mathbf{E}_0\omega\mathbf{E}_{\bar{0}}\mathbf{H}_1(y) \\ &= T_x \cdot \begin{pmatrix} 1 & 0 \\ \lambda & 1 \end{pmatrix} \begin{pmatrix} 0 & \lambda^{-1/2} \\ \lambda^{1/2} & 0 \end{pmatrix} \begin{pmatrix} 1 & 1/\lambda \\ 0 & 1 \end{pmatrix} \begin{pmatrix} y^{1/2} & 0 \\ 0 & y^{-1/2} \end{pmatrix} \cdot T_y \\ &= T_x \cdot \Phi(\lambda) \cdot YT_y \end{aligned} \tag{4.2}$$

with

$$\begin{aligned} \Phi(\lambda) &= \mathbf{E}_0\omega\mathbf{F}_0 = \begin{pmatrix} 0 & 1/\sqrt{\lambda} \\ \sqrt{\lambda} & \sqrt{\lambda} + 1/\sqrt{\lambda} \end{pmatrix} \\ \omega &= \sqrt{\lambda}\Lambda = \begin{pmatrix} 0 & 1/\sqrt{\lambda} \\ \sqrt{\lambda} & 0 \end{pmatrix}, \qquad \omega^2 = \mathbf{1}. \end{aligned} \tag{4.3}$$

For the $\widehat{SL(3)}$ system, corresponding to the graph $\Downarrow^{y_0\,\leftarrow\,x_1}_{x_0\,\rightarrow\,y_1}\Uparrow^{\rightarrow\,y_2}_{\leftarrow\,x_2}\Downarrow^{\leftarrow x_0}_{\rightarrow\,y_0}$ (i.e. glued with a vertical twist), instead of (4.1) we have to consider the three-product $\Xi(x_0, y_1)\Xi(x_1, y_2)\Xi(x_2, y_0)$, which is just a particular case of the generic $\widehat{SL(N)}$ expression

$$\Xi(x_0, y_1)\Xi(x_1, y_2) \ldots \Xi(x_{N-1}, y_N). \tag{4.4}$$

It is more convenient to rewrite (4.4) in new variables

$$\begin{aligned} x_i &= \frac{\xi_i}{\xi_{i+1}}, \qquad y_i = \frac{\eta_i}{\eta_{i+1}}, \qquad i = 1, \ldots, N-1 \\ \xi_N &= \xi_0, \qquad \eta_N = \eta_0 \end{aligned} \tag{4.5}$$

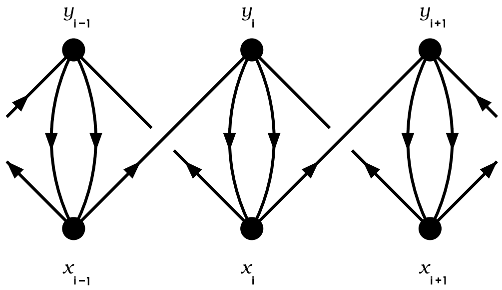

Fig. 5. Diagrammatic representation of the product of Ξ-operators in (4.4).

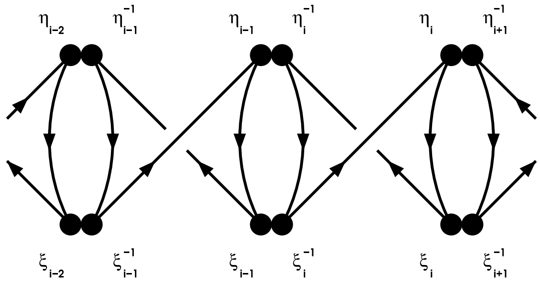

Fig. 6. The product of Ξ-operators becomes the product of L-matrices in (4.8) after a change in the variables.

so that the Poisson brackets (3.18) are now induced by

$$\{\eta_i, \xi_j\} = \delta_{ij}\eta_i\xi_j, \quad i,j = 1,\dots,N \tag{4.6}$$

and no restriction is immediately imposed on the products $\prod_{j=1}^N \xi_j$ and $\prod_{j=1}^N \eta_j$ (corresponding to the $GL(N)$ instead of the $SL(N)$ group, relating dynamic variables to the basis vectors of N-dimensional space; see the notation in Appendix A). Similar to (3.36), the coordinates and momenta $\{q_i, p_j\} = \delta_{ij}$ for (4.6) are introduced by

$$\begin{aligned} &\xi_i = \exp(-q_i), \qquad \eta_i = \exp(P_i + q_i), \quad i = 1,\dots,N \\ &P_i = p_i + \frac{\partial}{\partial q_i}\left(\frac{1}{2}\sum_{k=1}^N \mathrm{Li}_2\left(-\exp(q_k - q_{k+1})\right)\right). \end{aligned} \tag{4.7}$$

The product of Ξ-operators in (4.4) (see Fig. 5), again up to cyclic permutation, can be rewritten as

$$\Xi(x_0, y_1)\Xi(x_1, y_2)\dots\Xi(x_{N-1}, y_N) \simeq \prod_{j=1}^N L(\eta_j, \xi_j; \lambda) = \mathcal{T}_N(\lambda) \tag{4.8}$$

since (Fig. 6)

$$\begin{aligned} \dots\Xi(x_{i-1}, y_i)\dots = \quad & \dots T_{x_{i-1}}\Phi(\lambda)\begin{pmatrix} y_i^{1/2} & 0 \\ 0 & y_i^{-1/2}\end{pmatrix} T_{y_i}\dots \\ \underset{(4.5)}{=} \; & \dots T_{\xi_{i-1}}T_{\xi_i}^{-1}\Phi(\lambda)\begin{pmatrix} \eta_i^{1/2} & 0 \\ 0 & \eta_i^{-1/2}\end{pmatrix}\begin{pmatrix} \eta_{i+1}^{-1/2} & 0 \\ 0 & \eta_{i+1}^{1/2}\end{pmatrix} T_{\eta_i}T_{\eta_{i+1}}^{-1}\dots \\ = \quad & \dots\begin{pmatrix} \eta_i^{-1/2} & 0 \\ 0 & \eta_i^{1/2}\end{pmatrix} T_{\eta_i}^{-1}T_{\xi_i}^{-1}\Phi(\lambda)\begin{pmatrix} \eta_i^{1/2} & 0 \\ 0 & \eta_i^{-1/2}\end{pmatrix} T_{\eta_i}T_{\xi_i}\dots, \end{aligned} \tag{4.9}$$

where the right-hand side has only the factors corresponding to the ith instance. This is another example of localisation of the projection to the loop group with trivial co-extension, and we construct here a Poisson submanifold in $\widehat{SL(2)}^\sharp \to \widehat{SL(2)}$, making this projection using the $GL(N)$ variables in (4.5).

It is clear from (4.9) that on the right-hand side of (4.8) we obtain the product of the matrices (cf. with [25,26])

$$\begin{aligned} L_j(\lambda) &= \left(\mathbf{H}_1(\eta_j)\mathbf{H}_0(\xi_j)\right)^{-1}\cdot\Phi(\lambda)\cdot\mathbf{H}_1(\eta_j)\mathbf{H}_0(\xi_j) \\ &= \begin{pmatrix} 0 & \sqrt{\dfrac{\xi_j}{\lambda\eta_j}} \\ \sqrt{\dfrac{\lambda\eta_j}{\xi_j}} & \sqrt{\dfrac{\lambda}{\eta_j\xi_j}} + \sqrt{\dfrac{\eta_j\xi_j}{\lambda}} \end{pmatrix} = \begin{pmatrix} 0 & \dfrac{e^{-P_j/2-q_j}}{\sqrt{\lambda}} \\ \sqrt{\lambda}e^{P_j/2+q_j} & \sqrt{\lambda}e^{-P_j/2} + \dfrac{e^{P_j/2}}{\sqrt{\lambda}} \end{pmatrix} \quad j = 1,\dots,N. \end{aligned} \tag{4.10}$$

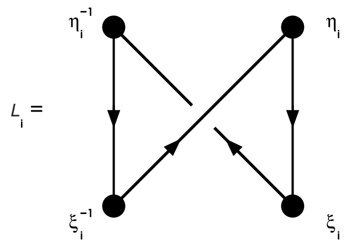

Fig. 7. Representation of the L-matrix from (4.10), which is a Cartan conjugation of (4.3) in the form of a twisted oriented plaquette.

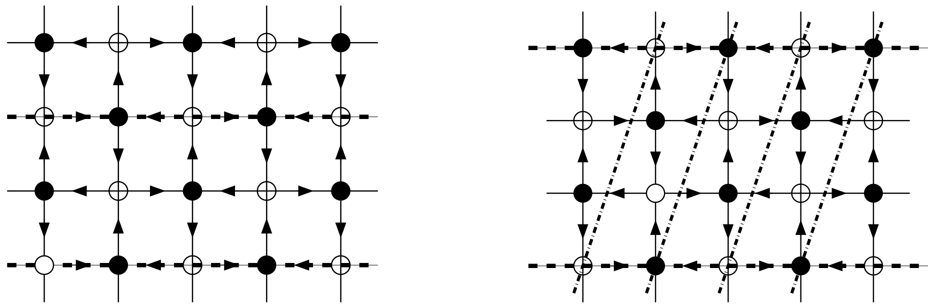

Fig. 8. Left: Contraction of an infinite square lattice by imposing a 2-periodicity constraint in the vertical direction, resulting in the graph $\cdots \rightleftarrows \Downarrow {}^{y_0}_{x_0} \begin{smallmatrix}\leftarrow\\ \rightarrow\end{smallmatrix} {}^{x_1}_{y_1} \Uparrow \begin{smallmatrix}\rightarrow\\ \leftarrow\end{smallmatrix} {}^{y_2}_{x_2} \Downarrow \cdots \Downarrow \begin{smallmatrix}\leftarrow\\ \rightarrow\end{smallmatrix} {}^{x_N}_{y_N} \Uparrow \begin{smallmatrix}\rightarrow\\ \leftarrow\end{smallmatrix} \cdots$. Right: Contraction of an infinite square lattice by imposing a 3-periodicity constraint in the vertical direction, together with an extra horizontal 1-step shift.

The dependence on dynamic variables arises from Cartan conjugation of the matrices (4.3) in the evaluation representation of $\widehat{SL(2)}$ (Fig. 7) and these L-matrices now obey the r-matrix Poisson relations

$$\left\{L_i(\lambda) \underset{,}{\otimes} L_j(\lambda')\right\} = -\frac{1}{2}\delta_{ij}\left[r_{\text{trig}}\left(\lambda, \lambda'\right), L_i(\lambda) \underset{,}{\otimes} L_j(\lambda')\right] \tag{4.11}$$

with the trigonometric classical r-matrix (B.9) (Appendix B). The same commutation relation obviously holds for the monodromy matrices (4.8),

$$\left\{\mathcal{T}_N(\lambda) \underset{,}{\otimes} \mathcal{T}_N(\lambda')\right\} = -\frac{1}{2}\left[r_{\text{trig}}\left(\lambda, \lambda'\right), \mathcal{T}_N(\lambda) \underset{,}{\otimes} \mathcal{T}_N(\lambda')\right]. \tag{4.12}$$

Therefore, their traces $\mathsf{T}_N(\lambda) = \operatorname{Tr} \mathcal{T}_N(\lambda)$, or the coefficients of the characteristic polynomial for the monodromy matrix

$$\det(\mathcal{T}_N(\lambda) + \mu) = \mu^2 + \mathsf{T}_N(\lambda)\mu + 1. \tag{4.13}$$

Poisson-commute $\{\mathsf{T}_N(\lambda), \mathsf{T}_N(\lambda')\} = 0$ with respect to (4.6) and generate $\lambda^{N/2}\mathsf{T}_N(\lambda) = \sum_{j=0}^{N} \lambda^j \tilde{R}_j(\boldsymbol{\xi}, \boldsymbol{\eta})$, the family of N independent integrals of motion:

$$\begin{aligned}
&\tilde{R}_0(\boldsymbol{\xi}, \boldsymbol{\eta}) = \prod_{k=1}^{N} \sqrt{\eta_k \xi_k} = \frac{1}{\tilde{R}_N(\boldsymbol{\xi}, \boldsymbol{\eta})} \\
&\tilde{R}_j(\boldsymbol{\xi}, \boldsymbol{\eta}) = \tilde{R}_0(\boldsymbol{\xi}, \boldsymbol{\eta})^{1-\frac{2j}{N}} \mathcal{H}_j(\mathbf{x}, \mathbf{y}), \quad j = 1, \ldots, N-1,
\end{aligned} \tag{4.14}$$

where the right-hand side has the Hamiltonians (3.34) as functions of the cluster variables (4.5).

4.2. $n \otimes N$ models from a square lattice

The formalism for a relativistic Toda in the previous section is based on construction of a Poisson submanifold in $\widehat{SL(2)}$, corresponding to a word of length $2N$. This has an obvious $n \otimes N$ generalisation (more strictly, $(n \times n)^{\otimes N}$; thus, $(2 \times 2)^{\otimes N}$ was considered in Section 4.1) to other co-extended loop groups.

A subclass of these systems can be constructed by gluing of the infinite-dimensional square lattice (Fig. 8) (V.V. Fock, unpublished data). For example, applying a 2-shift to the horizontal lines in such a lattice yields a graph consisting of two horizontal sets of vertices connected by vertical double edges (Fig. 8 left). After imposing an extra N-periodicity in the horizontal direction (for $N \geq 2$, with an extra twist for the odd N) we recover a construction of the monodromy matrix (4.8) for an affine Toda chain. The Poisson structure (3.31) is then induced by the Poisson structure on the lattice, determined by single arrows between neighbouring (black and white) vertices, drawn so that they follow the orientation of each plaquette of the lattice.

Some generalisations of the Toda models naturally arise for different gluings of the same lattice. For example, consider a 3-periodicity (instead of 2-periodicity) in the vertical direction, with an extra 1-step horizontal shift to be consistent with the orientation of the arrows (Fig. 8 right). Such a 3-reduced lattice can be further used for construction of the monodromy matrix in terms of the co-extended $\widehat{SL(3)}^\sharp$ loop group. We present this construction in the next section (of course, this is easily generalised to the loop groups $\widehat{SL(n)}^\sharp$ for any $n \geq 2$).

The Poisson structure given by the gluing shown on the right of Fig. 8 can be written as

$$\begin{aligned} \{y_j, x_i\} &= y_j x_i \quad \text{if } j = i \text{ or } j = i+3, \\ \{y_j, x_i\} &= -y_j x_i \quad \text{if } j = i+1 \text{ or } j = i+2 \end{aligned} \tag{4.15}$$

for some labelling with y values as the white vertices and x values as the black ones, while all the other brackets vanish. Another useful representation [28] for the same Poisson structure

$$\begin{aligned} \{Y_k, Y_{k\pm1}\} &= \mp Y_k Y_{k\pm1} \\ \{X_k, X_{k\pm1}\} &= \pm X_k X_{k\pm1} \end{aligned} \tag{4.16}$$

comes after the substitution

$$x_i = Y_i X_{i+1}, \qquad y_i = (X_{i-1} Y_{i-1})^{-1}. \tag{4.17}$$

The variables in (4.15) and (4.16) were already introduced in the context of an integrable system related to the pentagram map [6,7,27]. We now demonstrate that this is a generalised Toda system in the sense of our approach [3,4].

4.3. Integrable system for $n = 3$

For $n = 3$, similarly to (4.2), we start with the product (V.V. Fock, unpublished data)

$$\Xi(y, x) = \mathbf{H}_0(y)\mathbf{E}_0 \Lambda \mathbf{E}_{\bar{0}} \mathbf{H}_2(x) \tag{4.18}$$

of the elements of $\widehat{SL(3)}^\sharp$, where we use the notations in (2.7)–(2.9). These generators are labeled modulo 3 (e.g. $\mathbf{H}_{-1}(z) = \mathbf{H}_2(z)$, etc.), while the coordinates are considered further as N-periodic, that is, $x_{i+N} = x_i$, $y_{i+N} = y_i$, for an arbitrary $N \geq 3$.

The product $\Xi(y_i, x_i) \cdots \Xi(y_j, x_j)$ can be transformed by taking all the automorphisms Λ to the right:

$$\begin{aligned} \Xi(y_i, x_i) \ldots \Xi(y_j, x_j) &= \mathbf{H}_0(y_i)\mathbf{E}_0\Lambda\mathbf{E}_{\bar{0}}\mathbf{H}_{-1}(x_i) \ldots \mathbf{H}_0(y_j)\mathbf{E}_0\Lambda\mathbf{E}_{\bar{0}}\mathbf{H}_{-1}(x_j) \\ &= \mathbf{H}_0(y_i)\mathbf{E}_0\mathbf{E}_{\bar{1}}\mathbf{H}_0(x_i)\mathbf{H}_1(y_{i+1})\mathbf{E}_1\mathbf{E}_{\bar{2}}\mathbf{H}_1(x_{i+1}) \ldots \mathbf{H}_{j-i-1}(y_j)\mathbf{E}_{j-i-1}\mathbf{E}_{\overline{j-i}}\mathbf{H}_{j-i-1}(x_j)\Lambda^{j-i+1}. \end{aligned} \tag{4.19}$$

Therefore, up to the power of Λ at the end, this expression is for a particular case of the map (2.2) [17]. It corresponds to the word $u = \alpha_0\bar{\alpha}_1\alpha_1\bar{\alpha}_2 \ldots \bar{\alpha}_{j-i}$, and the corresponding exchange graph is equivalent to Fig. 8 (right), giving rise to the Poisson bracket (4.15).

Consider now a generic factor in the product (4.18) using coordinates (4.17)

$$\begin{aligned} \ldots \Xi(y_k, x_k; \lambda) \ldots = &\quad \ldots \mathbf{H}_0(y_k)\mathbf{E}_0\Lambda\mathbf{F}_0\mathbf{H}_2(x_k) \ldots \\ \underset{(4.17)}{=} &\quad \ldots H_2(Y_{k-1}X_k) T_{Y_{k-1}X_k} T^{-1}_{X_{k-1}Y_{k-1}} \Phi(\lambda) H_2(Y_k X_{k+1}) T_{Y_k X_{k+1}} T^{-1}_{X_k Y_k} \ldots, \end{aligned} \tag{4.20}$$

where

$$\Phi(\lambda) = \mathbf{E}_0\Lambda\mathbf{F}_0 = \begin{pmatrix} 0 & 0 & \lambda^{-1} \\ 1 & 0 & \lambda^{-1} \\ 0 & 1 & 1 \end{pmatrix} \tag{4.21}$$

and on the right-hand side or (4.20) we explicitly present all operators depending on the variables $\{Y_k, X_k\}$ at the kth site. This can be further rewritten as

$$\begin{aligned} &\ldots \underbrace{H_2(X_k) T_{X_k} \Phi(\lambda) T^{-1}_{X_k} H_2(Y_k)}_{k} \;\; \underbrace{H_2(X_{k+1}) \ldots}_{k+1} \;\; \ldots \\ &= \ldots \underbrace{H_2(X_k) \Phi(\lambda X_k) H_2(Y_k)}_{k} \;\; \underbrace{H_2(X_{k+1}) \ldots}_{k+1} \;\; \ldots, \end{aligned} \tag{4.22}$$

that is, as a product of the matrices (instead of the original operators (4.18) from $\widehat{PGL(3)}^\sharp$)

$$L_k(\lambda) = L(\lambda; X_k, Y_k) = H_2(X_k)\Phi(\lambda X_k)H_2(Y_k) = \begin{pmatrix} 0 & 0 & 1/\lambda \\ X_k Y_k & 0 & 1/\lambda \\ 0 & Y_k & 1 \end{pmatrix}, \tag{4.23}$$

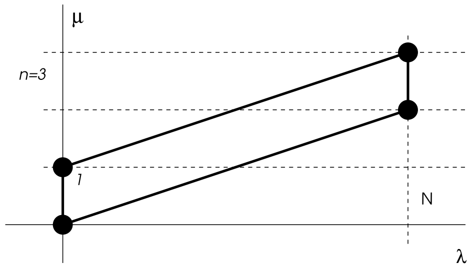

Fig. 9. Newton polygon for the curve (4.25), which leads to the genus formula (4.27).

each corresponding to a particular kth site. Using (4.20) and (4.22), the initial formula (4.19), up to cyclic permutations, is equivalent to the product

$$\Xi(y_0, x_0)\dots\Xi(y_{N-1}, x_{N-1}) \simeq \mathcal{T}_N(\lambda) = L_0(\lambda)\dots L_{N-1}(\lambda). \tag{4.24}$$

Note that on the right-hand side we again have the localised product of the matrices from $\widehat{PGL(3)}$, all with trivial co-extension, achieved here using the coordinates (4.16).

The characteristic polynomial for (4.24),

$$\lambda^N \det(\mathcal{T}_N(\lambda) + \mu) = \mu^3\lambda^N + \mu^2 C_2(\lambda) + \mu C_1(\lambda) + 1, \tag{4.25}$$

gives the spectral curve equation. The determinant of (4.24),

$$\lambda^N \det \mathcal{T}_N(\lambda) = \lambda^N \prod_{j=0}^{N} \det L_j(\lambda) = \prod_{j=0}^{N} X_j \left(\prod_{j=0}^{N} Y_j\right)^2 = 1, \tag{4.26}$$

is proportional to a Casimir function for (4.16) and is fixed to unity in (4.25). The coefficients of the polynomials $C_i(\lambda)$, $i = 1, 2$, in (4.25) are integrals of motion (and some of them are Casimirs in the even n cases), which Poisson-commute according to our general reasoning in Section 2. The genus of the curve (4.25) is always

$$g = 2\left(\left[\frac{N+1}{2}\right] - 1\right) = \begin{cases} 2\left[\frac{N}{2}\right], & N \text{ odd} \\ 2\left(\left[\frac{N}{2}\right] - 1\right), & N \text{ even}, \end{cases} \tag{4.27}$$

which can easily be seen from the corresponding Newton polygon in Fig. 9.

Example. For $N = 3$,

$$C_2(\lambda) = \lambda^3 + \lambda^2\mathcal{H}_2, \qquad C_1(\lambda) = -1 + \lambda\mathcal{H}_1 \tag{4.28}$$

with the Poisson-commuting Hamiltonians ($X_0X_1X_2 = 1$, $Y_0Y_1Y_2 = 1$)

$$\begin{aligned} \mathcal{H}_1 &= X_1 + X_2 + X_1X_2Y_1 + \frac{Y_2}{X_1} + \frac{1}{X_1X_2} + \frac{1}{X_2Y_1Y_2} \\ \mathcal{H}_2 &= Y_1 + Y_2 + X_2Y_1Y_2 + \frac{X_1}{Y_2} + \frac{1}{Y_1Y_2} + \frac{1}{X_1X_2Y_1} \end{aligned} \tag{4.29}$$

with respect to

$$\{\log X_1, \log X_2\} = 1 = \{\log Y_2, \log Y_1\}. \tag{4.30}$$

In symmetric form, (4.25) can be rewritten as

$$\begin{aligned} &w + \frac{1}{w} = z^{-3/2}P_3(z), \qquad w = (-\mu)^{1/2}\lambda^{3/2},\ z = -\mu\lambda \\ &P_3(z) = z^3 - \mathcal{H}_2 z^2 + \mathcal{H}_1 z - 1 \end{aligned} \tag{4.31}$$

and acquires the form of spectral curve (3.34) for the relativistic $\widehat{SL(3)}$ Toda chain.[2]

[2] To avoid misunderstanding, note that for $N = 3$ the spectral variables in (3.33) and (4.25) are related by $\lambda \leftrightarrow \lambda$, but $\mu \leftrightarrow \mu \cdot \lambda$. This transformation maps the Newton polygons in Figs. 3 and 9 to each other.

Rewriting (4.29) in the cluster coordinates $y_{i+3} = y_i$ and $x_{i+3} = x_i$, using

$$\begin{aligned} X_1 &= y_1 \prod_{k=1,2} (y_k x_k)^{-C^{-1}_{1k}}, \qquad X_2 = y_1 x_1 y_2 \prod_{k=1,2} (y_k x_k)^{-C^{-1}_{1k}} \\ Y_1 &= x_1 x_2 \prod_{k=1,2} (y_k x_k)^{-C^{-1}_{2k}}, \qquad Y_2 = y_1 y_2 x_2 \prod_{k=1,2} (y_k x_k)^{-C^{-1}_{2k}}, \end{aligned} \tag{4.32}$$

we return to (3.42). For $N = 4$ we obtain from (4.25)

$$\begin{aligned} C_2(\lambda) &= \lambda^4 + \lambda^3 \mathcal{H}_2 + \lambda^2 K_2(\mathbf{Y}) \\ C_1(\lambda) &= 1 - \lambda \mathcal{H}_1 + \lambda^2 K_2(\mathbf{X}) \end{aligned} \tag{4.33}$$

with $K_2(\mathbf{X}) = X_1X_3 + \frac{1}{X_1X_3}$ and the same for $K_2(\mathbf{Y})$, while

$$\begin{aligned} \mathcal{H}_1 &= X_1 + X_2 + X_3 + X_2X_1Y_1 + X_3X_2Y_2 + \frac{Y_3}{X_1X_2} + \frac{1}{Y_1Y_2Y_3X_2X_3} + \frac{1}{X_1X_2X_3} \\ &= X_1 + \frac{1}{X_1} + X_2 + \frac{1}{X_2} + X_1X_2Y_1 + \frac{1}{X_1X_2Y_1} + \frac{X_2Y_2}{X_1} + \frac{X_1}{Y_2X_2} \\ \mathcal{H}_2 &= Y_1 + Y_2 + Y_3 + Y_1Y_2X_2 + Y_2Y_3X_3 + \frac{X_1}{Y_2Y_3} + \frac{1}{X_1X_2X_3Y_1Y_2} + \frac{1}{Y_1Y_2Y_3} \\ &= Y_1 + \frac{1}{Y_1} + Y_2 + \frac{1}{Y_2} + Y_1Y_2X_2 + \frac{1}{Y_1Y_2X_2} + \frac{Y_2}{X_1Y_1} + \frac{X_1Y_1}{Y_2}, \end{aligned} \tag{4.34}$$

where the right-hand sides are obtained by fixing $K_2(\mathbf{X}) = K_2(\mathbf{Y}) = 2$. These Hamiltonians Poisson-commute with respect to the same bracket (4.30) as in the $N = 3$ case. The spectral curve (4.26) becomes

$$\mu^3\lambda^4 + \mu^2(\lambda^4 + \lambda^3\mathcal{H}_2 + 2\lambda^2) + \mu(1 - \lambda\mathcal{H}_1 + 2\lambda^2) + 1 = 0. \tag{4.35}$$

For $N \geq 5$ these formulas give rise to an integrable system related to the pentagram map [6,7]. In fact, (4.18) is the spectral-parameter-dependent Lax matrix for this system proposed by V.V. Fock (unpublished data) by relating it to the co-extended loop group (another Lax representation has been found in [10] and [9]).

5. Conclusion

We have demonstrated that relativistic Toda systems [13] arise naturally on the Poisson submanifolds in Lie groups. Extension of the construction from simple Lie groups to co-extended loop groups not only gives rise to their periodic versions, but also allows us to consider a much wider class of integrable models [3]. We discussed just a few particular examples whose phase spaces can be identified with Poisson manifolds obtained by regular gluing of a two-dimensional square lattice; more examples and a general formulation are available in the literature [3,4].

The proposed construction of the Poisson submanifolds in loop groups gives rise to their spectral curve equations and explicit formulas for the coefficients, the integrals of motion (corresponding usually to the internal points of their Newton polygons) in cluster variables. These formulas have a similar structure to partition functions of the dimer models, and this is not a coincidence. There is indeed a direct relation between the class of integrable systems arising from the dimer models on bipartite graphs on a torus [5] and those constructed from affine Lie groups. For any convex Newton polygon we can construct a wiring diagram on a torus and, after cutting the torus, an element from the co-extended double Weyl group [4]. On one hand this gives a Poisson submanifold in a loop group and an integrable system by the Lax map described above; on the other hand, each wiring diagram gives a bipartite graph on a torus, so that the face dimer partition function produces the same integrals of motion as the coefficients of the spectral curve equation.

We have also left for further research the quantum versions of our integrable models, which are beyond the scope of this paper. It has already been noted [2] that quantisation of the Toda chain can easily be done using the proposed approach by passing from classical to quantum groups, since the problem is identical to deformation of the algebra of functions $Fun(G)$ on group G [29–32]. Note that in cluster language the quantisation appears to be especially simple, since the Poisson brackets (2.4) are always logarithmically constant.

Finally, we point out that representatives of the family of integrable systems we consider here have many applications in mathematical physics; in particular, they are responsible for the Seiberg–Witten exact solutions to theories with explicitly present compact extra dimensions [22–24]. We expect a nontrivial relation between the cluster formulation of these integrable models and recently discussed cluster mutations, arising as generating transformations for the BPS spectra and being related to the wall-crossing phenomenon [33–35]. We are going to return to these issues elsewhere.

Acknowledgments

I am grateful to A. Braverman, B. Dubrovin, N. Early, S. Kharchev, S. Khoroshkin, I. Krichever, O. Kruglinskaya, A. Morozov, P. Pyatov, P. Saponov, M. Shapiro, and A. Zabrodin for useful discussions and to V. Fock for fruitful collaborations over many years of thinking about the subject of this paper. I would like to thank the University of Aarhus, the Max Planck and Haussdorf Institutes for Mathematics in Bonn, and the University of Strasbourg, where essential parts of this work were carried out. This work was partly supported by RFBR grant 11-01-00962, by joint RFBR project 12-02-92108, by the Program of Support of Scientific Schools (NSh-3349.2012.2) and by the Russian Ministry of Education under the contract 8498.

Appendix A. Roots, weights, and Cartan matrices

For $\mathfrak{g} = sl_N$ Lie algebras the Cartan matrix is

$$C_{ij} \underset{sl_N}{=} (\alpha_i \cdot \alpha_j) = 2\delta_{ij} - \delta_{i+1,j} - \delta_{i,j+1} \tag{A.1}$$

for the positive simple roots $\alpha_i \in \Pi$, $i, j = 1, \dots, \operatorname{rank} G = N - 1$. The dual vectors

$$(\mu_i \cdot \alpha_j) = \delta_{ij} \tag{A.2}$$

are the highest weights of the fundamental representations π_{μ_i}. Clearly,

$$\alpha_i = \sum_{j\in\Pi} C_{ij}\mu_j, \qquad \mu_i = \sum_{j\in\Pi} C^{-1}_{ij}\alpha_j. \tag{A.3}$$

It is convenient to use the weight vectors of the first fundamental representation

$$\nu_i = \mu_i - \mu_{i-1}, \quad i = 1, \dots, N, \tag{A.4}$$

for which $\mu_0 = \mu_N = 0$ is implied (i.e. $\nu_1 = \mu_1$ and $\nu_N = -\mu_{N-1}$), with the scalar products

$$(\nu_i \cdot \nu_j) = \delta_{ij} - \frac{1}{N}, \quad i, j = 1, \dots, N. \tag{A.5}$$

Vectors (A.4) are easily presented as a projection of the Cartesian basis vectors in N-dimensional vector space to a hyperplane, orthogonal to the vector $\frac{1}{N}\sum_{j=1}^N \mathbf{e}_j$:

$$\nu_i = \mathbf{e}_i - \frac{1}{N}\sum_{j=1}^N \mathbf{e}_j, \quad i = 1, \dots, N. \tag{A.6}$$

Comparing (A.3) and (A.4) and using (A.6), we find that

$$\alpha_i = \nu_i - \nu_{i+1} = \mathbf{e}_i - \mathbf{e}_{i+1}, \quad i = 1, \dots, N-1. \tag{A.7}$$

Recall that given a Cartan matrix C_{ij}, the Lie algebra $\mathfrak{g}$ is generated by $\{h_i | i \in \Pi\}$ and $\{e_i | i \in \Pi \cup \bar{\Pi}\}$ subject to the relations[3]

$$\begin{aligned} &[h_i, h_j] = 0, \qquad [h_i, e_j] = \operatorname{sign}(j) C_{ij} e_j, \qquad [e_i, e_{-i}] = \operatorname{sign}(i) h_i, \\ &(\operatorname{Ad} e_i)^{1-C_{ij}} e_j = 0 \quad \text{for } i + j \neq 0. \end{aligned} \tag{A.8}$$

We can also replace the set $\{h_i\}$ by the dual set $\{h^i\}$ by $h_i = \sum_{j\in\Pi} C_{ij} h^j$, so that

$$\begin{aligned} &[h^i, h^j] = 0, \qquad [h^i, e_j] = \operatorname{sign}(j) \delta^j_i e_j, \qquad [e_i, e_{-i}] = \operatorname{sign}(i) C_{ij} h^j, \\ &(\operatorname{Ad} e_i)^{1-C_{ij}} e_j = 0 \quad \text{for } i + j \neq 0. \end{aligned} \tag{A.9}$$

For any $i \in \Pi \cup \bar{\Pi}$ we can introduce the group element $E_i = \exp(e_i)$ and a one-parameter subgroup $H_i(z) = \exp(\log z \cdot h^i)$.

In the case of the affine Lie algebra $\mathfrak{g} = \widehat{sl}_N$, the set of simple roots is extended to $\alpha_i \in \Pi = \mathbb{Z}_N$ in a cyclically symmetric way and the Cartan matrix

$$\hat{C}_{ij} \underset{\widehat{sl}_N}{=} 2\delta_{ij} - \delta_{i+1,j} - \delta_{i,j+1}, \quad i, j \in \mathbb{Z}_N \tag{A.10}$$

is degenerate.

[3] To simplify them we extend h and C to negative index values, assuming that $h_i = h_{-i}$ and that $C_{-i,-j} = C_{ij}$ and $C_{ij} = 0$ if i and j have different signs, and using the notation $e_{-i} = e_{\bar{i}}$ for $i > 0$.

Appendix B. r-Matrices and Yang–Baxter equations

The classical limit of the Yang–Baxter equation

$$\hat{R}_{12}\hat{R}_{13}\hat{R}_{23} = \hat{R}_{23}\hat{R}_{13}\hat{R}_{12} \tag{B.1}$$

for $\hat{R}_{ij} = \exp\left(\hbar\, \hat{r}_{ij}\right)$ at $\hbar \to 0$ has the form

$$\left[\hat{r}_{12}, \hat{r}_{13}\right] + \left[\hat{r}_{12}, \hat{r}_{23}\right] + \left[\hat{r}_{13}, \hat{r}_{23}\right] = 0. \tag{B.2}$$

This can be solved, for example, by

$$\hat{r} = r_+ = \sum_{\alpha\in\Delta_+} (e_\alpha \otimes e_{\bar{\alpha}} + \mathbf{h}\otimes\mathbf{h}) \underset{sl_2}{=} e\otimes\bar{e} + \frac{1}{4} h\otimes h, \tag{B.3}$$

where (in the fundamental representation of sl_2)

$$e = \begin{pmatrix} 0 & 1 \\ 0 & 0 \end{pmatrix}, \qquad \bar{e} = \begin{pmatrix} 0 & 0 \\ 1 & 0 \end{pmatrix}, \qquad h = \begin{pmatrix} 1 & 0 \\ 0 & -1 \end{pmatrix} \tag{B.4}$$

and by

$$\hat{r} = r_- = \sum_{\alpha\in\Delta_+} (e_{\bar{\alpha}} \otimes e_\alpha + \mathbf{h}\otimes\mathbf{h}) \underset{sl_2}{=} \bar{e}\otimes e + \frac{1}{4} h\otimes h \tag{B.5}$$

obtained from (B.3) by the involution $e_\alpha \leftrightarrow e_{\bar{\alpha}}$ for $\alpha \in \Delta_+$ and $\mathbf{h} \leftrightarrow -\mathbf{h}$, preserving the commutation relations. The anti-symmetric r-matrix

$$r = e\otimes\bar{e} - \bar{e}\otimes e = \begin{pmatrix} 0 & 0 & 0 & 0 \\ 0 & 0 & 1 & 0 \\ 0 & -1 & 0 & 0 \\ 0 & 0 & 0 & 0 \end{pmatrix} = r_+ - r_- \tag{B.6}$$

satisfies the modified classical Yang–Baxter equation; for example, explicit calculation for (B.6) gives

$$[r_{12}, r_{13}] + [r_{12}, r_{23}] + [r_{23}, r_{13}] = h\wedge e\wedge \bar{e}, \tag{B.7}$$

which is enough to guarantee the Jacobi identity for the Poisson bracket (2.1).

In the case of loop algebras the corresponding $\hat{r}$-matrices acquire spectral parameter dependence corresponding to the evaluation representations of the corresponding current algebras [36]. Direct application of the anti-symmetric formula (3.1) for $\mathfrak{g} = \widehat{sl}_2$ gives rise to

$$\begin{aligned}
\sum_{\alpha\in\Delta_+} e_\alpha\wedge e_{\bar{\alpha}} &= \sum_{n\geq 0} e_n\wedge \bar{e}_{-n} + \sum_{n\geq 1}\left(\bar{e}_n\wedge e_{-n} + \frac{1}{2} h_n\wedge h_{-n}\right) \\
&= -\frac{\lambda+\lambda'}{\lambda-\lambda'}\left(e\otimes\bar{e} + \bar{e}\otimes e + \frac{1}{2} h\otimes h\right) + e\otimes\bar{e} - \bar{e}\otimes e \\
&= -\frac{\lambda+\lambda'}{\lambda-\lambda'}\begin{pmatrix} \frac{1}{2} & 0 & 0 & 0 \\ 0 & -\frac{1}{2} & 1 & 0 \\ 0 & 1 & -\frac{1}{2} & 0 \\ 0 & 0 & 0 & \frac{1}{2} \end{pmatrix} + \begin{pmatrix} 0 & 0 & 0 & 0 \\ 0 & 0 & 1 & 0 \\ 0 & -1 & 0 & 0 \\ 0 & 0 & 0 & 0 \end{pmatrix} \\
&= \begin{pmatrix} 0 & 0 & 0 & 0 \\ 0 & \frac{\lambda+\lambda'}{\lambda-\lambda'} & -\frac{2\lambda'}{\lambda-\lambda'} & 0 \\ 0 & -\frac{2\lambda}{\lambda-\lambda'} & \frac{\lambda+\lambda'}{\lambda-\lambda'} & 0 \\ 0 & 0 & 0 & 0 \end{pmatrix} - \frac{1}{2}\frac{\lambda+\lambda'}{\lambda-\lambda'}\,\mathbf{1}\otimes\mathbf{1}.
\end{aligned} \tag{B.8}$$

The expression on the right-hand side up to the part proportional to the unity operator, which does not contribute to any commutators, acquires the form

$$r_{\rm trig}(\lambda,\lambda') = \begin{pmatrix} 0 & 0 & 0 & 0 \\ 0 & \dfrac{\lambda+\lambda'}{\lambda-\lambda'} & -\dfrac{2\lambda'}{\lambda-\lambda'} & 0 \\ 0 & -\dfrac{2\lambda}{\lambda-\lambda'} & \dfrac{\lambda+\lambda'}{\lambda-\lambda'} & 0 \\ 0 & 0 & 0 & 0 \end{pmatrix} \tag{B.9}$$

in the Poisson bracket relations (4.11) in the context of 2×2 formalism. In the rational limit, with $\lambda = i\exp(\zeta/2)$ and small ζ, we obtain from (B.9)

$$r_{\rm trig}\left(ie^{\zeta/2}, ie^{\zeta'/2}\right) \underset{\zeta,\zeta'\to 0}{=} \frac{2}{\zeta-\zeta'}\begin{pmatrix} 0 & 0 & 0 & 0 \\ 0 & 1 & -1 & 0 \\ 0 & -1 & 1 & 0 \\ 0 & 0 & 0 & 0 \end{pmatrix} + \cdots. \tag{B.10}$$

Adding to the right-hand side the "unit" term $-\frac{2}{\zeta-\zeta'}\mathbf{1}\otimes\mathbf{1}$, we obtain in this limit $r_{\rm trig}\left(ie^{\zeta/2}, ie^{\zeta'/2}\right) \underset{\zeta,\zeta'\to 0}{=} -2r_{\rm rat}(\zeta,\zeta')$, where

$$r_{\rm rat}(\zeta,\zeta') = \frac{1}{\zeta-\zeta'}\begin{pmatrix} 1 & 0 & 0 & 0 \\ 0 & 0 & 1 & 0 \\ 0 & 1 & 0 & 0 \\ 0 & 0 & 0 & 1 \end{pmatrix} = \frac{1}{\zeta-\zeta'}\left(\frac{1}{2}\left(\mathbf{1}\otimes\mathbf{1} + h\otimes h\right) + e\otimes\bar e + \bar e\otimes e\right) \tag{B.11}$$

is the rational r-matrix proportional to the permutation operator in the tensor product $\mathbb{C}^2\otimes\mathbb{C}^2$.

Appendix C. Poisson structure on group manifolds

C.1. Graphs and Poisson brackets

Consider a graph (or a quiver) Γ comprising a set of $|\Gamma|$ vertices connected by an arbitrary number of oriented edges. Assign to each vertex $I\in\Gamma$ a (complex or real) variable z_I, $I = 1,\ldots,|\Gamma|$, to be thought of as coordinates on a chart in some manifold, mapped onto $\left(\mathbb{C}^\times\right)^{|\Gamma|}$. On such an open chart we can define the Poisson bracket (2.4) as [17]

$$\{z_I, z_J\} = \varepsilon_{IJ} z_I z_J, \qquad I, J = 1,\ldots,|\Gamma|, \tag{C.1}$$

where ε_{IJ} for the exchange matrix is

$$\varepsilon_{IJ} = \#\text{arrows}\,(I\to J) - \#\text{arrows}\,(J\to I). \tag{C.2}$$

Obviously, $\varepsilon_{IJ} = -\varepsilon_{JI}$ and the Jacobi identity is satisfied for (C.1) automatically. Moreover, exchange matrix (C.2) can even be non-integer-valued (e.g. half-integer).

The Poisson manifolds thus defined (see [17] and references therein for details) allow several operations that preserve the Poisson structure:

- For any subset $\Gamma'\subset\Gamma$ we can set

$$\varepsilon_{IJ'} = 0 \quad \forall I\in\Gamma,\ \forall J'\in\Gamma', \tag{C.3}$$

which corresponds to "forgetting" all vertices of Γ with the variables $\{z_{J'}\}$, $J'\in\Gamma'$.

- Gluing: for two graphs Γ_1 and Γ_2 *identify* their subsets $\Gamma_1' = \Gamma_2' = \Gamma'$, getting a graph

$$\Gamma = \Gamma_1\cup\Gamma_2 = \Gamma_1\diagdown\Gamma_1' \cup \Gamma' \cup \Gamma_2\diagdown\Gamma_2' \tag{C.4}$$

with the variables $z_{I_1} = z^{(1)}_{I_1}$ in all vertices $I_1\in\Gamma_1\diagdown\Gamma_1'$, $z_{I_2} = z^{(2)}_{I_2}$ for $I_2\in\Gamma_2\diagdown\Gamma_2'$, and $z_{I'} = z^{(1)}_{I'} z^{(2)}_{I'}$ for the coinciding $I'\in\Gamma'$. One gets then for the exchange matrix of (C.4)

$$\begin{aligned} &\varepsilon_{I_kJ} = \varepsilon^{(k)}_{I_kJ}, \quad J\in\Gamma, \qquad I_k\in\Gamma_k\diagdown\Gamma_k', \quad k = 1,2 \\ &\varepsilon_{I'J'} = \varepsilon^{(1)}_{I'J'} + \varepsilon^{(2)}_{I'J'}, \quad I', J'\in\Gamma'. \end{aligned} \tag{C.5}$$

- The Poisson structure (C.1) (for the *integer-valued* ε_{IJ}) is preserved by *mutations* of the graph and corresponding transformation of the z-variables according to

$$\mu_J:\ z_J \to \frac{1}{z_J}, \qquad z_I \to z_I\left(1+z_J^{\mathrm{sgn}(\varepsilon_{IJ})}\right)^{\varepsilon_{IJ}}, I \neq J. \tag{C.6}$$

This allows us to extend the bracket from an open chart to some globally defined cluster variety [14–16].

For certain graphs the Poisson structure (C.1) becomes equivalent to the r-matrix Poisson structure (2.1) on Lie groups, since it becomes possible to define the group-theoretical multiplication on certain graphs [17]. We illustrate this for a few particular examples.

C.2. Graphs and groups

1. The simplest graph $y \to x$ corresponds to the subgroup of upper-triangular matrices in $SL(2)$ or $PGL(2)$ (sometimes it is easier to forget about the determinant). More strictly, consider this as shorthand notation for

$$y \xrightarrow[E]{} x = YEX = \begin{pmatrix} y & 0\\ 0 & 1\end{pmatrix}\begin{pmatrix} 1 & 1\\ 0 & 1\end{pmatrix}\begin{pmatrix} x & 0\\ 0 & 1\end{pmatrix} = \begin{pmatrix} yx & y\\ 0 & 1\end{pmatrix} \tag{C.7}$$

with the matrix on the right-hand side considered as an element of $PGL(2)$. Consider a multiplication $(y \to x)\cdot(w \to z) = y \to xw \to z$ according to the gluing rule. After mutation at the intermediate point, the variables according to (C.6) transform to

$$xw \to \frac{1}{xw}, \qquad y \to y(1+xw) = \tilde{y}, \qquad z \to z\left(1+\frac{1}{xw}\right)^{-1} = \tilde{z}, \tag{C.8}$$

which corresponds to the second graph in Fig. 10, with the extra arrow between $\tilde{y}$ and $\tilde{z}$ reflecting that

$$\begin{aligned}\{\tilde{y},\tilde{z}\} &= \left\{y(1+xw),\, z\left(1+\frac{1}{xw}\right)^{-1}\right\}\\ &= (1+xw)z\left\{y, \left(1+\frac{1}{xw}\right)^{-1}\right\} + y\left(1+\frac{1}{xw}\right)^{-1}\{(1+xw), z\}\\ &= yxwz = \tilde{y}\tilde{z}.\end{aligned} \tag{C.9}$$

Forgetting the intermediate vertex, as in Fig. 10, we obtain the original graph $\tilde{y} \to \tilde{z}$ but with the new variables at the vertices. The rule for obtaining them exactly is

$$\begin{aligned}\left(y \xrightarrow[E]{} x\right)\cdot\left(w \xrightarrow[E]{} z\right) &= \begin{pmatrix} yx & y\\ 0 & 1\end{pmatrix}\begin{pmatrix} wz & w\\ 0 & 1\end{pmatrix} = \begin{pmatrix} yxwz & y(1+xw)\\ 0 & 1\end{pmatrix}\\ &= \begin{pmatrix} \tilde{y}\tilde{z} & \tilde{y}\\ 0 & 1\end{pmatrix} = \tilde{Y}E\tilde{Z} = \tilde{y} \xrightarrow[E]{} \tilde{z},\end{aligned} \tag{C.10}$$

corresponding to multiplication of the upper-triangular matrices. Normalising (C.7) to be an element of $SL(2)$ according to

$$y \xrightarrow[E]{} x = YEX = \begin{pmatrix} \sqrt{yx} & \sqrt{\dfrac{y}{x}}\\ 0 & \dfrac{1}{\sqrt{yx}}\end{pmatrix} \in SL(2), \tag{C.11}$$

we find that the Poisson bracket $\{y, x\} = yx$ exactly coincides with the restriction of the $SL(2)$ r-matrix Poisson bracket (2.1) to the triangular subgroup generated by the only positive root $E = \exp(e)$.

2. Consider now (C.7) as an upper-triangular subgroup of $SL(3)$ generated by any of the simple roots $E_i = \exp(e_i)$ and the Cartan elements $H_i(z) = \exp(\log z \cdot h^i)$, $i = 1, 2$. Using (3.1) we can easily compute the corresponding Poisson brackets; for example, for the matrix elements of

$$\begin{aligned}H_1(y)E_1H_1(x)H_2(z) &= \begin{pmatrix} y^{2/3} & 0 & 0\\ 0 & y^{-1/3} & 0\\ 0 & 0 & y^{-1/3}\end{pmatrix}\cdot\begin{pmatrix} 1 & 1 & 0\\ 0 & 1 & 0\\ 0 & 0 & 1\end{pmatrix}\begin{pmatrix} x^{2/3} & 0 & 0\\ 0 & x^{-1/3} & 0\\ 0 & 0 & x^{-1/3}\end{pmatrix}\begin{pmatrix} z^{1/3} & 0 & 0\\ 0 & z^{1/3} & 0\\ 0 & 0 & z^{-2/3}\end{pmatrix}\\ &= \begin{pmatrix} y^{2/3}x^{2/3}z^{1/3} & y^{2/3}z^{1/3}x^{-1/3} & 0\\ 0 & z^{1/3}y^{-1/3}x^{-1/3} & 0\\ 0 & 0 & y^{-1/3}x^{-1/3}z^{-2/3}\end{pmatrix}\end{aligned} \tag{C.12}$$

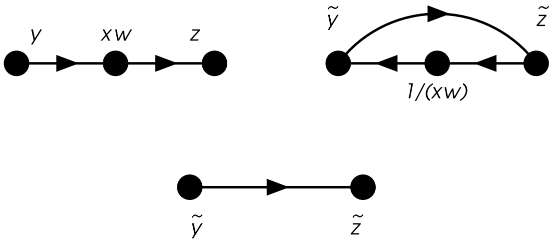

Fig. 10. Simplest graph and Lie group. Gluing, mutation at the middle point and forgetting this vertex after mutation give rise to the group multiplication law for the upper-triangular subgroup of $SL(2)$.

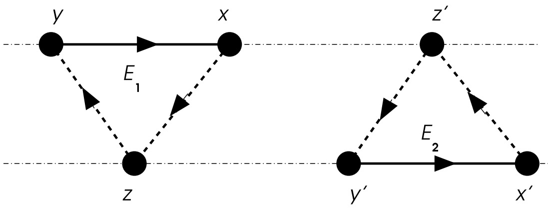

Fig. 11. Exchange graphs corresponding to the subgroups of $SL(3)$ generated by positive simple roots 1 (left) and 2 (right). The variables at vertices at the upper and lower levels parameterise the Cartan subgroups H_1 and H_2, respectively.

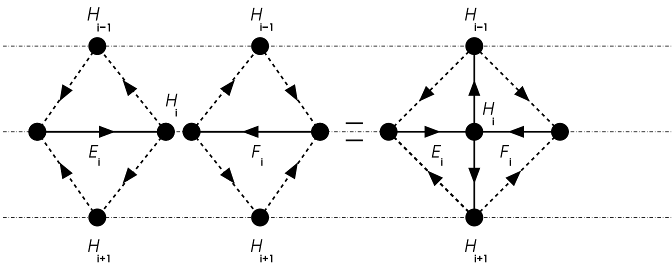

Fig. 12. Graphs depicting the subgroups of $SL(N)$ generated by the simple positive root E_i and negative root $E_{\bar{i}}$, $1 < i < N-1$. The variables at the vertices on each level correspond to the Cartan generators H_i and $H_{i\pm1}$. Gluing of two such graphs yields an element of the two-dimensional square lattice corresponding to a Poisson submanifold in $SL(N)$.

we obtain the Poisson relations

$$\{y, x\} = yx, \qquad \{x, z\} = \frac{1}{2}xz, \qquad \{z, y\} = \frac{1}{2}zy, \tag{C.13}$$

which can be represented by the left-hand graph in Fig. 11, with the dashed arrows connecting z to y and x.

Similarly, for the subgroup generated by the second root

$$H_2(y')E_2H_2(x')H_1(z') = H_1(z')H_2(y')E_2H_2(x') \tag{C.14}$$

we obtain the right-hand graph in Fig. 11, producing the same Poisson relations (C.13) for the prime variables. Almost the same triangles correspond to the subgroups generated by the negative roots $E_{\bar{1}}$ and $E_{\bar{2}}$; we only have to change the orientation of all the arrows in the plots.

The same arguments show that for simple roots of $SL(N)$ the corresponding subgroups are generated by *rhombi* instead of triangles (Fig. 12). The half-arrows on these rhombi are of the same nature as in Fig. 11, coming from the half-integer coefficients in (2.1). Gluing of two such rhombi at the ith level yields an element of the square lattice (Fig. 12). The symplectic leaves in $SL(N)$ can be constructed by further gluing of the elements from Fig. 12 (Fig. 1). In this way we obtain some particular gluing of the two-dimensional square lattice, among which is the Toda symplectic leaf in $SL(N)$ of dimension $2 \cdot \mathrm{rank}\, SL(N) = 2(N-1)$.

Appendix D. Toda theory from Lie algebra

In the case of Lie algebra instead of (2.1) we have the linear Poisson bracket

$$\left\{\mathcal{L} \underset{,}{\otimes} \mathcal{L}\right\} = -\frac{1}{2}\left[r, (\mathcal{L} \otimes 1 + 1 \otimes \mathcal{L})\right] \tag{D.1}$$

with the same constant r-matrix (3.1). For $GL(2)$ or $SL(2)$ it has only two non-vanishing entries (B.6), giving the following Poisson bracket relations for $\mathcal{L} = \begin{pmatrix} a & b \\ c & d \end{pmatrix} \in gl_2$:

$$\begin{aligned} &\{a, a\} = 0, \qquad \{a, b\} = -\frac{1}{2}b, \qquad \{a, c\} = -\frac{1}{2}c, \qquad \{a, d\} = 0 \\ &\{b, c\} = 0, \qquad \{b, d\} = -\frac{1}{2}b, \qquad \{c, d\} = -\frac{1}{2}c, \end{aligned} \tag{D.2}$$

which reflect the structure of the dual Lie algebra ($\mathrm{Tr}\mathcal{L} = a + d$ is now the Casimir function, the total momentum). The Darboux variables are introduced via

$$\mathcal{L} = \begin{pmatrix} a & b \\ c & d \end{pmatrix} = \begin{pmatrix} p & e^{q/2} \\ e^{q/2} & -p \end{pmatrix} \in sl_2, \qquad \{q, p\} = 1 \tag{D.3}$$

and the canonical Hamiltonian is given by $H = H_2 = \frac{1}{2}\mathrm{Tr}\,\mathcal{L}^2 = p^2 + e^q$.

In general, a Lie-algebraic-valued matrix of the form

$$\mathcal{L} = (p \cdot h) + \sum_{i \in \Pi} \left(e_i + e_{\bar{i}}\right) \exp(\alpha_i \cdot q) \tag{D.4}$$

satisfies (D.1) and produces Hamiltonians of the Toda system in a standard manner by computing invariant functions of (D.4). If the sum in (D.4) is taken over the set $\Pi \subset \Delta_+$ of positive simple roots for the finite-dimensional Lie algebra, we obtain the open Toda chain, whereas for the affine Lie algebra with e_i and $e_{\bar{i}}$ values taken in the evaluation representation, we obtain the spectral-parameter-dependent Lax operator for the periodic Toda chain.

In the context of alternative 2×2 formalism, in the algebraic limit (roughly, linear in momenta, exponential coordinates and ζ, if $\lambda = i\exp(\zeta/2)$) then the Lax matrix (4.10) becomes

$$\frac{1}{i} \begin{pmatrix} 0 & \dfrac{e^{-P_j/2 - q_j}}{\sqrt{\lambda}} \\ \sqrt{\lambda} e^{P_j/2 + q_j} & \sqrt{\lambda} e^{-P_j/2} + \dfrac{e^{P_j/2}}{\sqrt{\lambda}} \end{pmatrix} \to L_j(\zeta) = \begin{pmatrix} 0 & -\exp\left(-q_j/2\right) \\ \exp\left(q_j/2\right) & \zeta - p_j \end{pmatrix} \quad j = 1, \ldots, N, \tag{D.5}$$

which satisfies the Poisson bracket [25]

$$\left\{ L_i(\zeta) \underset{,}{\otimes} L_j(\zeta') \right\} = \delta_{ij} \left[r_{\mathrm{rat}}\left(\zeta, \zeta'\right), L_i(\zeta) \underset{,}{\otimes} L_j(\zeta') \right] \tag{D.6}$$

with the rational r-matrix (B.11).

References

[1] M. Olshanetsky, A. Perelomov, Invent. Math. 37 (1976) 93.
[2] V.V. Fock, A. Marshakov, A note on quantum groups and relativistic Toda theory, Nuclear Phys. B 56 (Suppl.) (1997) 208–214.
[3] V.V. Fock, A. Marshakov, Lie groups, Toda chains and cluster variables, Report ITEP/TH-12/11, FIAN/TD-03/11, 2011.
[4] V.V. Fock, A. Marshakov, Integrable systems, cluster variables and dimers (in preparation).
[5] A. Goncharov, R. Kenyon, Dimers and cluster integrable systems, Preprint. arXiv:1107.5588.
[6] V. Ovsienko, R. Schwartz, S. Tabachnikov, The pentagram map: a discrete integrable system, Comm. Math. Phys. 299 (2010) 409–446.
[7] V. Ovsienko, R. Schwartz, S. Tabachnikov, Liouville–Arnold integrability of the pentagram map on closed polygons, Preprint. arXiv:1107.3633.
[8] M. Gekhtman, M. Shapiro, A. Vainshtein, Generalized Backlund–Darboux transformations for Coxeter–Toda flows from a cluster algebra perspective, Acta Math. 206 (2011) 245–310.
[9] M. Gekhtman, M. Shapiro, S. Tabachnikov, A. Vainshtein, Higher pentagram maps, weighted directed networks, and cluster dynamics, Prepint. arXiv:1110.0472.
[10] F. Soloviev, Integrability of the pentagram map, Preprint. arXiv:1106.3950.
[11] R. Eager, S. Franco, K. Schaeffer, Dimer models and integrable Systems, J. High Energy Phys. 1206 (2012) 106.
[12] H. Williams, Double Bruhat cells in Kac–Moody groups and integrable systems, Lett. Math. Phys. (in press). http://dx.doi.org/10.1007/s11005-012-0604-3.
[13] S. Ruijsenaars, Comm. Math. Phys. 133 (1990) 217.
[14] S. Fomin, A. Zelevinsky, Cluster algebras I: foundations, J. Amer. Math. Soc. 15 (2002) 497–529.
[15] A. Berenstein, S. Fomin, A. Zelevinsky, Cluster algebras III: upper bounds and double Bruhat cells, Duke Math. J. 126 (2005) 1–52.
[16] V.V. Fock, A.B. Goncharov, Moduli spaces of local systems and higher Teichmuller theory, Publ. Math. Inst. Hautes Études Sci. 103 (2006) 1–211.
[17] V.V. Fock, A.B. Goncharov, Cluster X-varieties, amalgamation and Poisson–Lie groups, Progr. Math. 253 (2006) 27–68.
[18] T. Hodges, T. Levasseur, Primitive ideals of $C_q[SL(3)]$, Comm. Math. Phys. 156 (1993) 561.
[19] T. Hoffman, J. Kellendonk, N. Kuntz, N. Reshetikhin, Factorization dynamics and Coxeter–Toda lattices, Comm. Math. Phys. 212 (2000) 297.
[20] V. Kac, Infinite-Dimensional Lie Algebras, Cambridge University Press.
[21] L. Faddeev, A. Volkov, Discrete evolution for the zero-modes of the quantum Liouville model, J. Phys. A 41 (2008) 194008.
[22] N. Nekrasov, Five-dimensional Gauge theories and relativistic integrable systems, Nuclear Phys. B 531 (1998) 323–344.
[23] A. Marshakov, A. Mironov, 5D and 6D supersymmetric Gauge theories: prepotentials from integrable systems, Nuclear Phys. B 518 (1998) 59.
[24] H.W. Braden, A. Marshakov, A. Mironov, A. Morozov, The Ruijsenaars–Schneider model in the context of Seiberg–Witten theory, Nuclear Phys. B 558 (1999) 371.
[25] L. Faddeev, L. Takhtadjan, Hamiltonian Approach to the Theory of Solitons, Nauka, 1986.

[26] Y. Suris, A collection of integrable systems of the Toda type in continuous and discrete time, with 2×2 Lax representations, Preprint. arXiv:solv-int/9703004.
[27] M. Glick, The pentagram map and Y-patterns, Adv. Math. 227 (2011) 1019–1045.
[28] R. Schwartz, Discrete monodromy, pentagrams, and the method of condensation, J. Fixed Point Theory Appl. 3 (2008) 379–409.
[29] V. Drinfeld, Quantum groups, in: Proceedings of the International Congress of Mathematicians, Berkeley, 1986, p. 798.
[30] M. Jimbo, A q-difference analogue of $U(g)$ and the Yang–Baxter equation, Lett. Math. Phys. 10 (1985) 63.
[31] N.Y. Reshetikhin, L.A. Takhtadzhyan, L.D. Faddeev, Quantization of Lie groups and Lie algebras, Algebra i Analiz 1 (1988) 128–206.
[32] L. Faddeev, N. Reshetikhin, L. Takhtadjan, Quantum groups, in: Braid Group, Knot Theory and Statistical Mechanics, World Scientific, 1989, p. 97.
[33] M. Kontsevich, Y. Soibelman, Stability structures, motivic Donaldson–Thomas invariants and cluster transformations, Preprint. arXiv:0811.2435.
[34] D. Gaiotto, G.W. Moore, A. Neitzke, Wall-crossing, Hitchin systems, and the WKB approximation, Adv. Math. 234 (2013) 239–403.
[35] M. Alim, S. Cecotti, C. Cordova, S. Espahbodi, A. Rastogi, C. Vafa, $N = 2$ quantum field theories and their BPS quivers, Preprint. arXiv:1112.3984.
[36] G. Arutyunov, Construction of trigonometric Toda r-matrices via Hamiltonian reduction of the cotangent bundle over loop groups, Theoret. Math. Phys. 113 (1997) 1209–1216.